

AN EXPERIMENTAL STUDY OF THE THERMAL CHARACTERISTICS OF A LAMINAR BUOYANT JET

By

S. SATYANARAYANA

ME

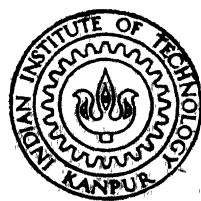
1979

TH
ME/1979/4
Sa 842.

M

S

EXP



DEPARTMENT OF MECHANICAL ENGINEERING
INDIAN INSTITUTE OF TECHNOLOGY, KANPUR
NOVEMBER, 1979

AN EXPERIMENTAL STUDY OF THE THERMAL CHARACTERISTICS OF A LAMINAR BUOYANT JET

**A Thesis Submitted
In Partial Fulfilment of the Requirements
for the Degree of
MASTER OF TECHNOLOGY**

By

S. SATYANARAYANA

**to the
DEPARTMENT OF MECHANICAL ENGINEERING
INDIAN INSTITUTE OF TECHNOLOGY, KANPUR
NOVEMBER, 1979**

ME-1978-M-SAT-EXP

I.I.T. KANPUR
CENTRAL LIBRARY
Acc. No. A 62160.
• 5 MAY 1988

ii)

12.11.79

21

CERTIFICATE

This is to certify that the thesis entitled
"An Experimental Study of the Thermal Characteristics of
A Laminar Buoyant Jet" by Mr. S. Satyanarayana is a record
of work carried out under my supervision and has not been
submitted elsewhere for a degree.



November, 1979

(YOGESH JALURIA)
Assistant Professor
Department of Mechanical Engineering
Indian Institute of Technology Kanpur
India

21.9.79 21

ACKNOWLEDGEMENTS

I wish to express my deep sense of gratitude to Dr. Yogesh Jaluria for his invaluable help and encouragement throughout the course of this work.

I am very thankful to Mr. P.N. Misra, for his assistance throughout the experimental work. I am very thankful to Mr. K. Himasekhar, for many fruitful discussions I had with him. My sincere thanks are also due to Mr. T. Premananda Reddy and all my friends who helped me directly and indirectly.

I thank Mr. R.K. Bajpai and Mr. J.C. Verma for their efficient tracing of the graphs, Mr. U.S. Misra for typing the thesis.

S. Satyanarayana
(S. SATYANARAYANA)

CONTENTS

		Page	
CHAPTER	1	INTRODUCTION	1
	1.1	Introduction to the Problem	1
	1.2	Review of Literature	3
	1.3	Present work	7
CHAPTER	2	Experimental Arrangement	9
CHAPTER	3	Experimental Results and Discussions	12
	3.1	Horizontal inflow	12
	3.2	Inclined inflow	17
	3.3	Vertical inflow	19
	3.4	Transient behaviour with inflow and outflow	22
CHAPTER	4	CONCLUSIONS	25
REFERENCES	:		27
FIGURES	:		29

LIST OF FIGURES

	Page	
Fig. 1	View of Perspex tank	29
Fig. 2	Schematic diagram of experimental arrangement	30
Fig. 3	Temperature profiles with inlet at the centre, with $\frac{Gr}{Re^2} = 0.119$, $Re = 375.4$, $Gr = 1.6739 \times 10^4$	31
Fig. 4	Temperature profiles with inlet at the centre, with $\frac{Gr}{Re^2} = 0.0594$, $Re = 530.6$, $Gr = 1.6739 \times 10^4$	32
Fig. 5	Temperature profiles with inlet at the centre, with $\frac{Gr}{Re^2} = 0.02048$, $Re = 904$, $Gr = 1.6739 \times 10^4$	33
Fig. 6	Temperature profiles with inlet at the centre, with $\frac{Gr}{Re^2} = 0.00887$, $Re = 1376$, $Gr = 1.6739 \times 10^4$	34
Fig. 7	Temperature profiles with inlet at the bottom, with $\frac{Gr}{Re^2} = 0.0687$, $Re = 530.6$, $Gr = 1.935 \times 10^4$	35
Fig. 8	Temperature profile, with inlet at the bottom, with $\frac{Gr}{Re^2} = 0.02368$, $Re = 904$, $Gr = 1.935 \times 10^4$	36
Fig. 9	Temperature profiles with inlet at the bottom, with $\frac{Gr}{Re^2} = 0.0594$, <u>$Re = 530.6$</u> , $Gr = 1.6739 \times 10^4$	37

Fig. 10	Temperature profiles with inlet at the bottom, $\frac{Gr}{Re^2} = 0.02048$, $Re = 904$, $Gr = 1.6739 \times 10^4$	38
Fig. 11	Temperature profiles in the transverse direction for inflow at the bottom, with $\frac{Gr}{Re^2} = 0.00887$, $Re = 1376$, $Gr = 1.6739 \times 10^4$	39
Fig. 12	Jet centre-line trajectory with inlet at the centre	40
Fig. 13	Jet centre-line trajectory with inlet at the bottom	41
Fig. 14	Comparison of the jet centre-line trajectory with inlet at the bottom and at the centre	42
Fig. 15	Temperature profiles when jet is inclined at 30° downward, with $\frac{Gr}{Re^2} = 0.02048$, $Re = 904$, $Gr = 1.6739 \times 10^4$	43
Fig. 16	Temperature profiles when jet is inclined at 30° downwards, with $\frac{Gr}{Re^2} = 0.00887$, $Re = 1376$, $Gr = 1.6739 \times 10^4$	44
Fig. 17	Temperature profiles when jet is inclined at 45° downwards, with $\frac{Gr}{Re^2} = 0.02048$, $Re = 904$, $Gr = 1.6739 \times 10^4$	45
Fig. 18	Temperature profiles when jet is inclined at 45° downwards, with $\frac{Gr}{Re^2} = 0.00887$, $Re = 1376$, $Gr = 1.6739 \times 10^4$	46

Fig. 19	Jet centre-line trajectory with different inclinations	47
Fig. 20	Temperature profiles for a vertical jet	48
Fig. 21	Centre-line temperature versus vertical height for a vertical buoyant jet	49
Fig. 22	Comparison between measured temperatures and the theoretical curve for a vertical buoyant jet	50
Fig. 23	Temperature profiles of the water body in the region of the jet with inflow at the bottom and outflow at the top on the opposite side of tank	51
Fig. 24	Transient behaviour of the water body above the jet when the inlet is at the bottom and the outlet at the top on the opposite side of the tank	52
Fig. 25	Temperature profiles of the water body in the region of the jet with inflow at the centre and outflow at the top on the opposite side of the tank	53
Fig. 26	Temperature profiles of the water body in the jet region when the inlet is at the centre and the outlet at the top on the opposite side of the tank	54

NOMENCLATURE

D,	Diameter of the jet;
f,	Non-dimensionalized stream function;
g,	Gravitational acceleration;
Gr,	Grashof number, (Gr = $\frac{g \Delta D (t_i - t_\infty)}{\nu^2}$);
J,	Momentum flux in the vertical direction, defined in section (3.3);
K,	constant, defined in section (3.3);
Re,	Reynolds number, (Re = $\frac{U_J D}{\nu}$);
T,	Dimensionless time;
t,	Temperature measured at any location in the water body;
t_i ,	Inlet temperature of the jet fluid;
t_∞ ,	Ambient fluid temperature;
t_o ,	Centre-line temperature of the jet;
U_J ,	Jet velocity at the inlet
$U_{\bar{x}}$,	velocity in vertical direction, defined in section (3.3);
\bar{x} ,	vertical distance, defined in section (3.3);
\bar{y} ,	Horizontal distance measured from the jet axis, defined in section (3.3);
$\frac{x}{D}$,	Non-dimensional horizontal distance measured in the central plane of the jet;
$\frac{y}{D}$,	Non-dimensional vertical distance measured in the central plane of the jet;

$\frac{z}{D}$, Dimensionless distance measured in the transverse direction

Greek Symbols

α , Thermal diffusity of fluid;

β , Coefficient of thermal expansion of fluid;

ϵ , Parameter, defined in section (3.3);

ζ , Similarity variable, defined in section (3.3);

δ , Boundary layer thickness;

ν , Kinematic viscosity of the fluid,

ϕ , Dimensionless temperature, ($\phi = \frac{t - t_{\infty}}{t_i - t_{\infty}}$);

$\tilde{\phi}$, Dimensionless temperature, ($\tilde{\phi} = \frac{t - t_{\infty}}{t_o - t_{\infty}}$);

ψ , Physical stream function, defined in section (3.3);

τ , Time measured in hours.

ABSTRACT

In the present work, an experimental investigation has been carried out to study the trajectory and other thermal characteristics of the jet flow driven by buoyancy and momentum input. A jet of hot water is injected into an enclosed water body, contained in a large tank. Temperatures, in the central plane of the jet, are measured. The jet trajectory, for various input conditions is obtained by plotting the location of the maximum temperature in the jet on an X-Y plane. In the first part of the thesis, horizontal inflow has been considered and the jet trajectory, for various values of the mixed convection parameter Gr/Re^2 and for different locations of the inlet, has been determined. Inclined jets are studied in the second part and their trajectory has been obtained. Vertical jets have also been studied and the centre-line temperature decay and the temperature profiles have been obtained. A comparison is also made with the analytical results to indicate interesting differences. In the last part, the transient behaviour of the temperature field in the water body has been studied with a horizontal inflow into the tank coupled with an outflow at the top. The basic features of the temperature field are determined in these cases. Interest lies in the trajectory, the jet spread and the temperature decay with height. These are important in heat removal and rejection systems. This study provided insight into many of these important considerations.

1. Introduction

1.1 Introduction to the Problem:

Flows commonly referred to as jets may be regarded as part of free boundary flows, i.e., flows characterized by the absence of rigid boundaries. The important input quantities, which determine the type of flow, for jets and plumes, are the momentum and heat input. The flow dominated by momentum input is termed as a jet and that by heat input as a thermal plume. It is also convenient to subdivide these flows on the basis of whether they are laminar or turbulent, buoyant or non-buoyant. A jet is buoyant if the discharged fluid is lighter than the ambient fluid, as is the case for the flow of hot fluid released in an extensive ambient medium at a lower temperature. Such flows are important in technology, meteorology, oceanography, pollution of air and water, buoyancy-driven ocean circulations and in the thermal recirculation in lakes resulting from hot water discharges.

In recent years, a considerable interest has been directed at the study of axissymmetric free turbulent jets, with regard to their various applications. When a turbulent jet of fluid is injected into surroundings of a different density, the buoyancy force acts on it and affects its momentum. As the jet flows downstream, its energy is gradually dispersed to the surroundings, through entrainment of

ambient fluid. The jet spreads out, increasing in diameter, downstream. Maximum velocity and temperature occur at the axis of jet. These features are exhibited by hot gas jets, such as those in furnaces, effluents from chimneys and cooling towers and thermal discharges into water bodies.

In literature, one aspect which has not received close attention is the influence of the initial difference between the jet temperature and that of the surroundings on the jet trajectory. Jets that issue horizontally into homogeneous denser ambient fluid are driven upwards by the buoyancy force. The axis is, therefore, a curve and the velocity and temperature at any point in the jet depends on the distance from the nozzle, measured along the axis of the jet, on the distance from the axis of jet, and on the input conditions, such as inflow velocity, temperature, etc., of the jet.

In recent years, increasing interest has been seen in the problem of the disposal of industrial waste and the discharge of hot water from cooling systems, of power stations, into water bodies. In the cooling water problem, the difference in the temperature between the warm water and the surrounding fluid, gives rise to buoyancy mechanisms, that result in mixed convection. Problems associated with environmental pollution require knowledge of the characteristics of

the buoyant jet, such as the decay of the centre-line velocity and temperature and the trajectory of the jet, if the buoyancy force and the initial direction of flow are not aligned. The effect of the initial density difference, between the jet and the surroundings, on the jet trajectory is of importance. If the buoyancy force and the initial direction of discharge are aligned, as in vertical jets, the flow is affected, though the trajectory remains vertical. An aiding buoyancy mechanism will increase the velocity and an opposing one will reduce it.

1.2 Review of Literature:

The first important study on jets was carried out by Schlichting (1933). Using boundary layer approximations, similarity solutions were found for both the two dimensional and axisymmetric jets. Bosarquet et.al. (1961) studied, experimentally and analytically, the effect of the initial density difference on the path of jets. They employed a water model technique, which was devised to represent the path taken by jets. In the model, a magnetic slurry jet, whose density was greater than that of the surrounding flowing stream of water in a large transparent box, was injected and photographed. They presented a theory for predicting the axis of jet in terms of the initial velocity, the density ratio, the nozzle diameter and the angle of inclination of the axis of projection.

They compared favourably this predicted axis of the jet with observed values obtained in the water model.

Abraham (1965) analysed the gross behaviour of turbulent buoyant jets, discharged horizontally, and compared the theory with the experimental results. The solution is based on the integral approach, assuming the velocity and temperature profiles to be Gaussian across the jet and integrating them over the jet cross section. Turner (1966) studied experimentally the motion of turbulent jets of heavy salt solution injected upwards into a tank of fresh water and compared the results with those of plumes which are initially buoyant but become heavy as they mix with the environment. Turner measured the penetration distance of salt water and expressed it as proportional to the mixed convection parameter, which compares natural convection effects to forced convection.

Several experiments have been performed on the mixing of turbulent water jets discharged into a body of receiving water. Jen et. al. (1966) carried out experiments to determine the characteristics of warm water circular jets discharged horizontally at the surface of a deep quiescent water body. They found an expression for the relationship between temperature and the distance along the jet axis at the water surface, for densimetric Froude number from 18 to 180. Measurements have been made on the shape of a plume of

warm water, for a similar range of conditions, by Wood and Wilkinson (1967). Circular jets were used with densimetric Froude number between 10 and 60.

Brand and Lahey (1967) investigated the problem of a heated jet discharged vertically upward from an orifice into a region of the same fluid. The boundary layer equations of both two-dimensional and axisymmetric jets, for the steady laminar flow of a vertical jet including the buoyancy term, are solved by the similarity method. They attempted to relate plume and jet flows. Anwar (1969) analytically determined the trajectory of plumes, assuming that the profiles of mean velocity and of excess buoyancy are of similar form, for all distances from the nozzle. This was also verified experimentally, using fresh water jets discharged in saline water. Investigations on buoyant jet discharged at the water surface are relevant to thermal pollution and industrial waste disposal, in which density stratification exercises an important effect on the flow and temperature fields.

The heated two-dimensional jet discharged at the water surface has also been studied. Wada (1968) carried out a theoretical analysis and calculated the velocity and temperature distributions. Miyazaki (1974) determined theoretically the flow and thermal characteristics, for varying nozzle exit Richardson number. He found that the total flow rate, or the stream function at the boundary edge, increases

with the dimensionless horizontal distance as expected.

Mollendorf and Gebhart (1973) have investigated the effect of a small amount of thermal buoyancy in round laminar vertical jets. A numerical solution of the resulting perturbation equations shows that the predominant effect of positive thermal buoyancy is to increase the axial velocity component of the jet and to thin the jet. Patton et. al. (1974) experimentally presented characteristics of a heated and unheated two-dimensional water jet injected into a moving water stream. They found that the jet trajectory as determined from the location of the maximum velocity does not change with jet temperature, at least for jet temperatures upto 4.5°C above the ambient. Hence, they concluded that the buoyancy force has negligible influence on the jet trajectory for a two-dimensional jet.

Yang and Patel (1973) presented the analysis of mixed natural and forced convection in a two-dimensional wall jet along a vertical isothermal wall. Pryputriewiez and Bearley (1975) presented an experimental study of turbulent buoyant jets discharged vertically through a single circular submerged pipe into a large body of stagnant unstratified water of finite depth. The centre-line and surface temperatures were obtained as functions of the discharge Froude number, ranging from 1 to 50, and of the discharge depth. They also presented the governing equations to predict the jet characteristics, using

integral analysis approach.

Recently Seban et.al. (1978) measured centre-line temperatures in a heated air jet discharged downward into an ambient air and showed that the centre-line temperature and the penetration distance are predicted adequately by the constant property theory for the downward flow alone. They also measured the radial temperature profiles and then estimated the width of the downward jet and concluded that the upward does influence the downward flow.

1.3 Present work:

As mentioned above, the effect of the initial density difference, between the jet and the surroundings, on the jet trajectory has not been studied in detail. In the present work, this aspect has been considered and the jet trajectory has been determined experimentally for various input conditions.

The experiment consists of a large tank containing tap water. A jet of hot water is injected horizontally from the inlet location on one side of this tank. Initially, no outflow is taken and the flow is in an extensive medium. The centre-line of the jet trajectory has been found out, considering the fact that, for this axisymmetric flow, the maximum velocity and the maximum temperature lie on the centre-line of the jet trajectory. Inlet positions are located at the centre and at the bottom on one side of the tank. With inlet at the centre of

tank, the temperatures in the jet central plane and jet trajectories are found out. With inlet at the bottom of the tank, the jet centre-line is found out at various values of the inlet velocity of the jet and of the inlet temperature of the jet. Temperatures in the transverse direction are also measured and the spread of the jet is determined.

In the second part of the experiment, inclined jets have been considered and the resulting trajectory has been determined. Vertical jets have also been studied experimentally and a comparison is made with the analytical work of Mollendorf and Gebhart (1973). The steady flow case was also carried out. The outlet was located at the top on the opposite side of the tank. The transient behaviour of the water body has been determined.

The study, therefore, focuses on the trajectory and on the characteristics of the jet flow driven by buoyancy and momentum input. Laminar flow is considered in this study. This would relate to low flow rates, such as those encountered for small heat rejection rates. Similar considerations also arise in energy storage, as sensible heat, e.g., in solar energy storage systems.

2. Experimental arrangement

To study the trajectory of the buoyant jet, water contained in a tank was employed. The tank was made of perspex and had inside dimensions of $0.6 \times 0.6 \times 0.4$ m, as shown in Figure 1. On one side of the tank, three circular holes were drilled. Brass tubes of internal diameter 0.6 cm. were inserted in these holes, and sealed against leakage. On the opposite side of the tank, an outflow opening was made at the top. This opening was used when out flow was considered. The tank was insulated on the four sides with thermocole sheets of thickness 0.025 m.

The water jet, heated by means of a constant temperature water heating bath, was discharged into the water contained in the tank. Water from an overhead tank flows through a coil placed inside the temperature bath. The hot water leaving the coil was discharged into the water body at any one of the desired inlet locations. The arrangement employed for the flow is shown in Figure 2. In order to vary and measure the hot water flow rates, a rotameter with a needle valve arrangement was fitted at one end of the tube, which carries the water through the temperature bath. The temperature of the hot water was varied by operating the thermo-regulator valve, which controls the temperature of the bath.

Temperatures in the water body were measured by means of thermocouples, employing a 48-channel Honeywell temperature recorder. The recorder has an accuracy of about 0.15°C . Copper-constantan thermocouples of gauge 24 were calibrated and used for the measurement of temperature. A thermocouple probe was made. Holes at a distance of 1 cm. were drilled along its length. These holes were used for locating the thermocouples. Starting from the bottom hole of the probe, nine thermocouples were placed, each at a distance of 1 cm. from the other. Beyond this distance, four thermocouples, each at a distance of 2 cm. from one another, were placed. In the remaining length of the probe, five more thermocouples, 5 cm. distance apart, were placed. These thermocouples were placed in the holes of the probe and protruded 1 cm from the probe. The thermocouple probe was fixed by means of a clamp to a rod attached to an iron stand. The stand could be moved horizontally, to measure the temperature, in the jet path. The horizontal distance was measured by means of a scale, fixed to the table, along which the stand carrying the thermocouple probe was moved. The vertical distance was determined by noting the distance between thermocouples and the height of the lowest thermocouple. The temperatures in the jet at any axial location were measured by this arrangement. Thermocouples were also located at the

inlet and the outlet positions, to measure the inlet and outlet temperatures.

3. Experimental Results and Discussions

3.1 Horizontal inflow:

The test tank was filled with tap water upto about 75% of its height. Hot water, at different flow rates, was injected into the tank from the centre inlet tube. Temperatures at various locations in the central plane of the jet were recorded. The above experimental procedure was repeated, with the inlet position located at the bottom of the tank. This experiment was done with different inlet temperatures and with different flow rates. Low flow rates were employed to ensure laminar flow. The experiment, therefore, considers the flow of buoyant jet in an extensive isothermal medium, since the level of water in the tank rises very gradually. The temperature in the ambient medium was monitored to ensure that no significant recirculation or stratification arises. The measurements were thus carried out in an extensive, quiescent isothermal medium.

The horizontal distances X and the vertical distances Y were non-dimensionalized with the inflow diameter of the jet. The temperatures were non-dimensionalized with the inlet temperature of the jet to yield the dimensionless temperature ϕ as :

$\phi = \frac{t - t_{\infty}}{t_i - t_{\infty}}$ where, t_{∞} is the ambient water temperature and t_i is the jet inlet temperature. The measured temperature profiles are plotted for various values of the parameter Gr/Re^2 , where Gr is the Grashof number and Re is the Reynolds number defined as:

$$Gr = \frac{g\beta D^3 (t_i - t_{\infty})}{\nu^2}$$

$$Re = \frac{U_J D}{\nu}$$

where, g is gravitational acceleration, β the coefficient of thermal expansion, ν the kinematic viscosity of the fluid and U_J the inlet velocity of the jet. The temperature profiles are shown in Figures 3 to 10.

In all these plots, a peak in the profiles is observed. The temperature approaches zero, away from the jet axis, towards the wall as expected. The location of the maximum temperature moves away from the inlet wall indicating the downstream flow of the jet. The maximum temperature decays with the horizontal distance X/D from the inlet, as may be expected from entrainment of ambient fluid. The thickness of the jet also increases as the jet moves away from the inlet due to this increased flow. An increase in the parameter Gr/Re^2 has a considerable effect on these profiles. From Figures 3 to 6, it is observed that the height above the inlet, at which maximum temperature occurs at given horizontal

locations, decreases as the rate of flow increases, indicating a more gradual upward flow of the jet at higher flow rates. At any location, the thickness of the jet also increases as the flow rate increases indicating larger entrainment. As the jet traverses away from the inlet, the vertical height above the inlet, at which zero temperature occurs, is increased as seen from Figure 4. At a particular horizontal location, the vertical distance above the jet, at which zero temperature occurs, decreases as the rate of flow increases, as seen from the Figures 3 to 6. This is largely due to the increase in momentum as flow increases and also due to larger entrainment of the surrounding fluid as the jet traverses downstream. Similar effects are seen at a larger inlet temperature, as shown in Figures 7-10.

The temperature profile in the transverse direction was also measured when a jet of hot water is injected from the bottom inlet position. The temperature profiles in the transverse direction are plotted in Figure 11. The thermal boundary layer thickness, defined in terms of the location at which temperature is 1% of the centre-line temperature difference from ambient, i.e., $\phi = 0.01$, is found from these plots. It is observed that the thermal boundary layer thickness increases as the jet moves away from the inlet. As the jet traverses forward, the mass of the moving fluid

increases, because of entrainment of surrounding fluid and, due to this, the jet spreads out. At any section, the spread of the jet is given by twice the thermal boundary layer thickness, due to symmetry. This measurement was made in the central plane of the jet.

The trajectory of the jet is obtained by plotting the location of the maximum temperature on an X-Y plane. This is shown for various values of Gr/Re^2 and for different inlet positions in Figures 12 & 13. Here the fact that, in axisymmetric jets, the maximum temperature occurs along the centre-line of the jet is employed. When a jet is injected into a quiescent isothermal surroundings, the input thermal energy of the jet is gradually dispersed due to the entrainment of ambient fluid. The input momentum is distributed over more fluid and velocity decreases. A buoyant jet of fluid, injected into a water body of different density, deviates from the inlet flow direction due to the action of the buoyancy force. This is evident from the Figures 12 and 13. The higher temperature of the jet fluid makes it lighter and this buoyant fluid, therefore, rises vertically. Ambient fluid is entrained as the jet moves away from the inlet and its temperature and velocity decrease while the mass of the moving fluid increases. It is observed from Figure 13 that, for a particular Re , as the Gr decreases, the jet goes further from the wall at a given vertical location. It is evident from Figure 13 that

as the Re increases, the horizontal distance travelled by the jet increases, due to the predominance of the momentum to buoyancy mechanisms initially. The jet traverses into the water body to the distance upto which a significant density difference exists. Beyond that, the jet fluid essentially mixes with the ambient fluid and temperature difference can not be measured accurately.

A comparison of the jet trajectory with inlet location at the bottom with that for the inlet at the centre, is also made, as shown in Figure 14. The flow conditions remaining the same, the jet goes further from the wall, at a given vertical distance, in the case of inlet location at the centre as compared to that for the bottom inlet location. When the jet is injected from the centre, the entrainment of surrounding fluid is more, compared to the jet injected from the bottom inlet, which is near to the bottom wall of the tank. The wall curbs entrainment due to the obstruction it offers. For inflow at the centre, the jet entrains on both sides and, hence, the entrainment is expected to be more. Due to this, the temperatures in the jet at a location are higher in the case of bottom inlet and the buoyancy force, which drives the jet vertically, is lesser in case of central inlet location.

3.2 Inclined inflow:

A central hole at an inclination of 45° downwards with the horizontal direction was made on a perspex sheet of dimensions $3 \times 3 \times 0.5$ cm. This sheet was then fitted to the inside wall of the tank at the central hole. Now the jet of hot water impinges at an inclination of 45° downwards. Hot water with different flow rates was injected into the tank from this inclined centre hole. Temperatures at various locations in the central plane of the jet were recorded. The above experiment was repeated with a 30° inclined hole. The measured temperatures are plotted for various values of the parameter Gr/Re^2 , as shown in Figures 15-18.

In these plots, a peak in the profile is observed as seen earlier. For a particular horizontal location, as the flow rate increases, the height below the inlet, at which maximum temperature occurs, increases. This is expected due to the increase in the downward momentum. As the jet crosses the horizontal plane passing through the inlet, the jet of fluid moves vertically and the height above the jet at which maximum temperature occurs becomes smaller as flow increases. The horizontal distance travelled by the jet increases as the rate of flow increases due to the predominance of momentum to buoyancy. At a particular horizontal location, in the region before the jet starts moving upwards, the depth below the jet

at which maximum temperature occurs increases, as the inclination of jet increases. It is evident from the Figures 15-18 that the maximum temperature at a particular horizontal location decreases, as the inclination of the jet increases, due to the downward motion of the jet, which makes the jet travel further for greater inclinations, before a given horizontal location is reached.

The trajectory of the jet is shown in Figure 19, for various values of the parameter Gr/Re^2 and for 45° and 30° inclinations. When a jet of hot water is discharged downwards into the ambient region, the jet initially flows downwards and then the flow reverses and traverses in upward direction. Initially the momentum in the downward direction dominates the buoyancy force and makes the jet to flow in the downward direction. The buoyancy force continues to act vertically upwards. Therefore it tries to generate momentum in the vertical direction. As the flow proceeds away from the inlet, the force acts on the jet flow and eventually turns the flow upwards. This is similar to the motion of a projectile ejected upward, at an angle with the ground. As inclination increases, the flow goes further downstream and thus in reaching a given horizontal location, it traverses a larger distance entraining more fluid. This is reflected in greater spread of the jet, lower temperature, as compared to smaller inclinations. The

trajectory indicates the nature of the anticipated temperature field. The measurement substantiate the physical aspects of the flow.

3.3 vertical inflow:

A copper tube elbow, bent at 90°, of 5 cm. length, 1 cm. height and 0.6 cm. inside diameter was kept tightly secured along its length in the groove of a heavy rubber cork. It was kept at a central location of the test tank. Inlet connection was made to this elbow to generate a vertical jet. Hot water, with different flowrates, was injected into the water body through this arrangement. Temperatures in the region of the jet were recorded.

Mollendorf and Gebhart (1973), in their analysis of laminar vertical jets, include the effect of buoyancy as a linear perturbation on the known closed form similarity solution for nonbuoyant jets. They solved the uncoupled problem, in terms of f and ϕ , defined as:

$$\psi = \omega \bar{x} f(\zeta),$$

$$\phi = \frac{t - t_{\infty}}{t_0 - t_{\infty}} \text{ and ,}$$

$$\zeta = \frac{\bar{y}}{\bar{x} \sqrt{K}}, \text{ where, } K = \frac{16}{3} \pi \rho \nu^2 / J.$$

Here J is the momentum flux in the vertical direction \bar{x} , and is

defined as:

$$J = \int_0^{\infty} 2\pi \rho \frac{U^2}{X} \bar{Y} d\bar{Y} = \text{constant}$$

where \bar{Y} is the distance from the jet axis measured in horizontal direction. They obtained f and ϕ as

$$f = \frac{\gamma^2}{1 + \frac{1}{4}\gamma^2} \quad \text{and} \quad \phi = (1 + \frac{1}{4}\gamma^2)^{-2} \text{Pr}, \text{ with,}$$

$$\gamma = \sqrt{\frac{3}{16\pi}} \frac{\sqrt{\bar{Y}/\rho}}{\bar{Y}} \frac{\bar{Y}}{X}$$

Similarity solution does not exist for the coupled problem due to the added thermal buoyancy term. It can thus be solved by perturbation techniques. The perturbation parameter $\epsilon(x)$ is given as

$$\epsilon(x) = \frac{Gr_x}{4}, \text{ where,}$$

$$Gr_x = \frac{g\beta \bar{X}^3 (t_0 - t_\infty)}{2^2} ; R = \frac{U_J D}{\bar{a} \gamma}$$

where \bar{X} has a value of 4.0 for a parabolic velocity profile. They found that the effect of thermal buoyancy, on the temperature is less significant than that on the velocity. The effect was small over the range considered.

In the above analysis, \bar{X} , the vertical distance, is measured from a point source. The distance between the actual finite sized source and a virtual, point source, which gives

the same flow, can be determined by assuming that at the actual source location, the boundary layer thickness, δ , would be equal to the radius of the circular source. The calculation for this is as follows:

$$\gamma = \sqrt{\frac{3}{16\pi}} \frac{\sqrt{J/\rho}}{D} \bar{y}/\bar{x}$$

$$\text{Therefore, } \bar{x} = \sqrt{\frac{3}{16\pi}} \frac{\sqrt{J/\rho}}{\gamma} \frac{\delta}{\gamma_{\text{edge}}}$$

From the above expression \bar{x} can be found. For the present experiment, \bar{x} was found to be equal to 1.34 meters. Adding this distance between the actual source and the virtual source, to the measured vertical distance above the jet, experimental γ is found. Now a comparison may be made between the analytical results and the experimental data. It was found that experimental results are of similar form but the actual profiles do not agree, as may be expected from the very different nature of flow mechanisms. For a smaller inlet diameter, the comparison may be expected to be better. In a distance of 1.34 meters, the flow actually undergo transition to turbulence. Thus the temperature field measured is quite different from the idealized theory.

The measured temperature profiles are plotted in Figure 20. The temperature at a point was found to increase as the flow rate, or Re , increases. This is also seen in terms of

the dimensionless temperature $\bar{\theta}$. Figure 21 shows the centre-line temperature decay with the vertical distance above the jet, for two different flow rates of Re is 2142 and Re is 1376. The slopes of the plotted curve on a log-log graph, is found to be -1.09 and -1.23 respectively. The first one is in close agreement with the theoretical value of -1.0, as given by Mollendorf and Gebhart (1973). As the jet moves upwards, due to the entrainment of the surrounding fluid, the centre-line temperature of the jet decreases. Figure 22 shows the plot of the non-dimensional temperature $\bar{\theta}$ versus \bar{y}/δ , for both experimental and theoretical results. Within the experimental limitations, the value of ϵ , the thermal buoyancy perturbation parameter, nearest to the theoretical value of 1.0 is found to be 1.39. It is evident from the Figure 22 that thermal buoyancy has a small effect on the form of the temperature profile. It does however, effect the temperature decay.

3.4 Transient behaviour with inflow and outflow:

The tank was completely filled with tap water. Hot water was continuously injected into the tank, from the bottom inlet position. Outflow was located at the top on the other side of the tank. Temperatures in the central plane of the jet and at different locations in the water body away from the jet, were recorded at various intervals of time. The above

experimental procedure was repeated with the central inlet also.

Temperature profiles are plotted as shown in Figures 23-26. It is observed from Figure 23 that the temperatures in the jet central plane goes in increasing with time as expected. It would attain steady state when inlet temperature is attained. The water body above the jet becomes isothermal and its temperature also gradually increases with time. From the measurements, it was observed that the trajectory of the jet was not altered very much, in the isothermal region though the temperatures, obviously, vary. In these profiles, a peak is observed at a particular location. This is due to the jet centre-line passing through that point at that particular horizontal location. At any point, beyond the region in which the jet traverses, the water body becomes isothermal and its temperature continues to increase with time, as shown in Figure 24. The water body becomes isothermal due to thermal diffusion and buoyancy effects that arise. Figure 25 shows the temperature profiles in the region of the traverse of the jet, when the inflow is located at the centre. As expected, a peak occurs at a point where the jet centre-line is located. Above the jet, the water body becomes isothermal, with increasing temperature as time progresses. Just below the jet, the temperature in the water

body increases very gradually and far away from the jet the water body becomes isothermal with only a slight increment in temperature from the initial ambient condition. This can be seen in Figure 25.

Most of the energy transfer occurs above the jet region and the water body attains higher temperatures compared to that in the region below the jet. At any point beyond the jet traverse region, the water body above the jet becomes isothermal with increasing temperature as time progresses. For below the inlet location, the water body becomes isothermal with low temperatures. The former is heating from below and the latter heating from above, with expected results. Below the inlet region, the water body temperature increases only due to the conduction of heat from the hotter fluid. A stable stratification exists in the water body as the lighter fluid lies above the heavier fluid.

4. Conclusions

From these experimental results, it is found that the trajectory of the jet depends on the location of the inlet position, on the inclination of the inflow, on the inlet temperature, on the rate of flow, on the density of the ambient region into which it is injected. As the jet of hot fluid traverses downstream its temperature decreases due to the entrainment of the surrounding fluid. The entrainment of the surrounding fluid increases as the rate of inflow is increased. The depth of penetration downwards of the jet depends on the angle of inclination of the jet and on the initial momentum and the inlet temperature. This factor is important in the discharge of hot water from the condensers of a power plant, or from industrial units, to the cooling water body. While moving downwards into the water body, the hot fluid loses energy rapidly and by the time it reaches the outflow location, its temperature has been drastically reduced. From the vertical inflow results, it may be noted that the thermal buoyancy has little effect on the form of the temperature profile, though the temperature level is affected significantly. When there is inflow and outflow, a stable stratification exists in the water body below the jet, as the lighter fluid lies above the heavier fluid. Initially, the water body behaves like an extensive medium to the jet of hot

fluid. But as time increases, the hot fluid flow may be regarded as internal flow and the temperature of the water body also increases. It may be expected that the horizontal penetration of the jet would decrease with increase in time. This study may be extended to study the jet characteristics in a stratified water body, which would apply after thermal discharge occurs over a significant time period. A consideration of turbulent jets is also desirable, since these are often of greater relevance to power plant discharges. The present work considers the basic features of the flow and indicates the nature of thermal field that arises.

REFERENCES

1. Abraham, G. (1965) "Horizontal jets in stagnant fluid of other density", J. Hyd. Div., ASCE, Vol. 91, pp.139-154.
2. Anwar, H. (1969), "Behaviour of Buoyant jet in a calm fluid", J. Hyd. Div. ASCE, Vol. 95, pp. 1289-1303.
3. Bosarquet, C.H., Horn, G and Thring, M.W. (1961), "The effect of Density difference on the path of jet", Proc. Roy. Soc. London, Vol. A263, p. 340.
4. Brand, R.S., and Lahey, F.J. (1967), "The heated laminar vertical jet", J. Fluid Mech., Vol. 29, pp. 305-315.
5. Jen, Y., Wiegel, R.L. and Mobark, I (1966), "Surface discharge of horizontal warm water jet," J. power Div., ASCE, Vol. 92, pp. 1-30.
6. Miyazaki, H (1974), "Heated Two Dimensional jet discharged at water surface", Int. J. Heat Mass Transfer, Vol. 17 pp. 1269-1272.
7. Mollendorf, J.C. and Gebhart, B. (1973), "Thermal buoyancy in round laminar vertical jets", Int. J. Heat Mass Transfer, Vol. 16, pp. 735-745.
8. Patton, A.J. and Test, F.L. (1974), "An experimental investigation of a heated two-dimensional water jet discharged into a moving stream, " J. Heat Transfer, Vol. 96, p. 273.

9. Pryputniewicz, R.J. and Bearly, W.W. (1975), "An experimental study of vertical buoyant jet discharged into water of finite depth", J. Heat Transfer, Vol. 97, pp. 274-281
10. Schlichiting, H (1933), "Laminar Strömungsbretung", Boundary Layer Theory, pp. 164-181, McGrawhill, 1968.
11. Seban, R.A. (1978), "Temperatures in a heated jet discharge downwards", Int. J. Heat mass Transfer, Vol. 21, pp. 1453-1458.
12. Yang, J.W. and Patel, R.D. (1973), "Effect of buoyancy on forced convection in a two-dimensional wall jet along a vertical wall", J. Heat Transfer, Vol. 95, pp. 121-123.
13. Turner, J.J. (1966), "Jets and Plumes with negative buoyancy", J. Fluid Mech., Vol. 26, pp. 779-792.
14. Wada, A. (1968), "Numerical analysis of distribution of flow and thermal diffusion caused by out fall of cooling water", Coastal Engineering, Japan, 11, pp. 161-173.

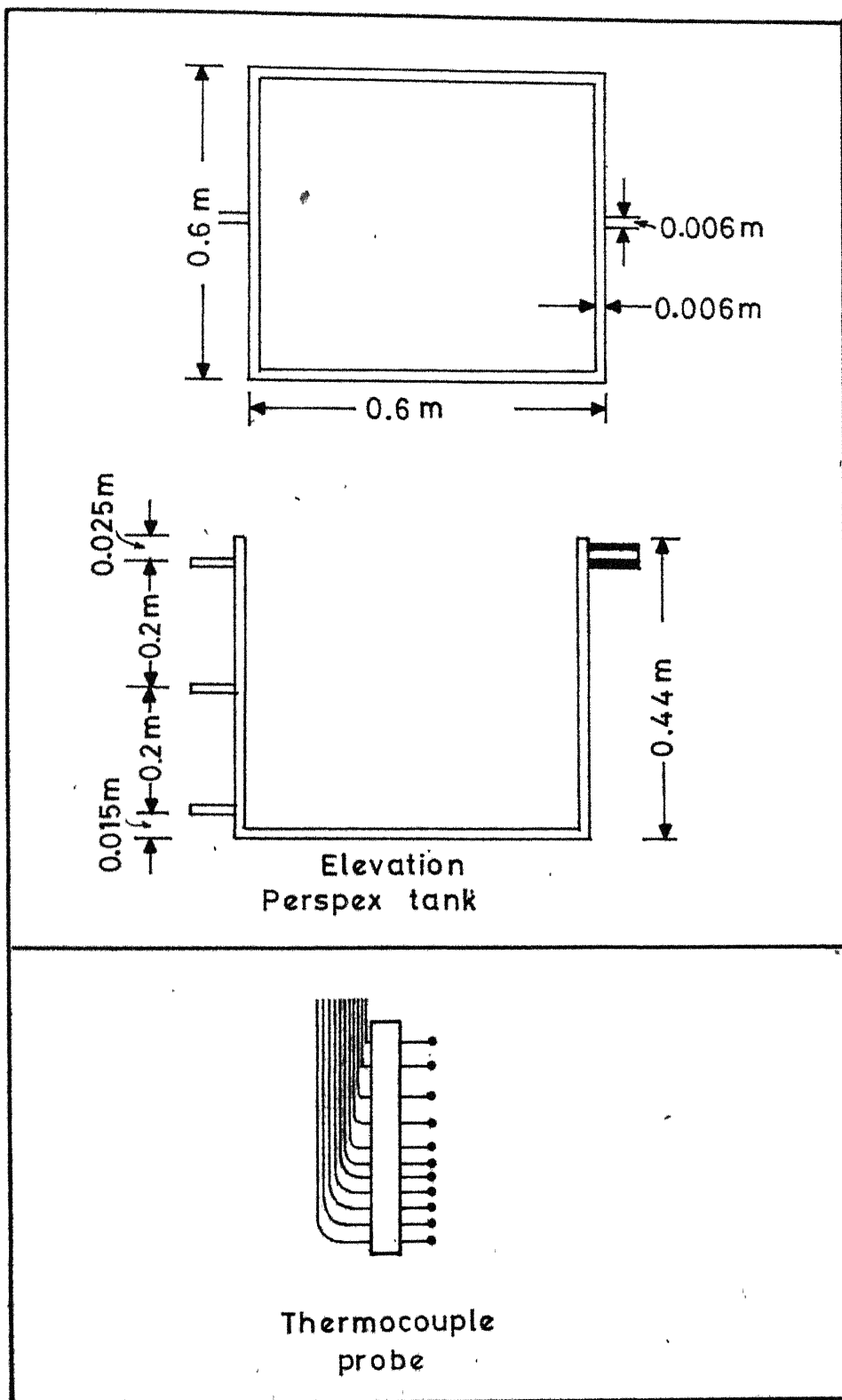


Fig. 1

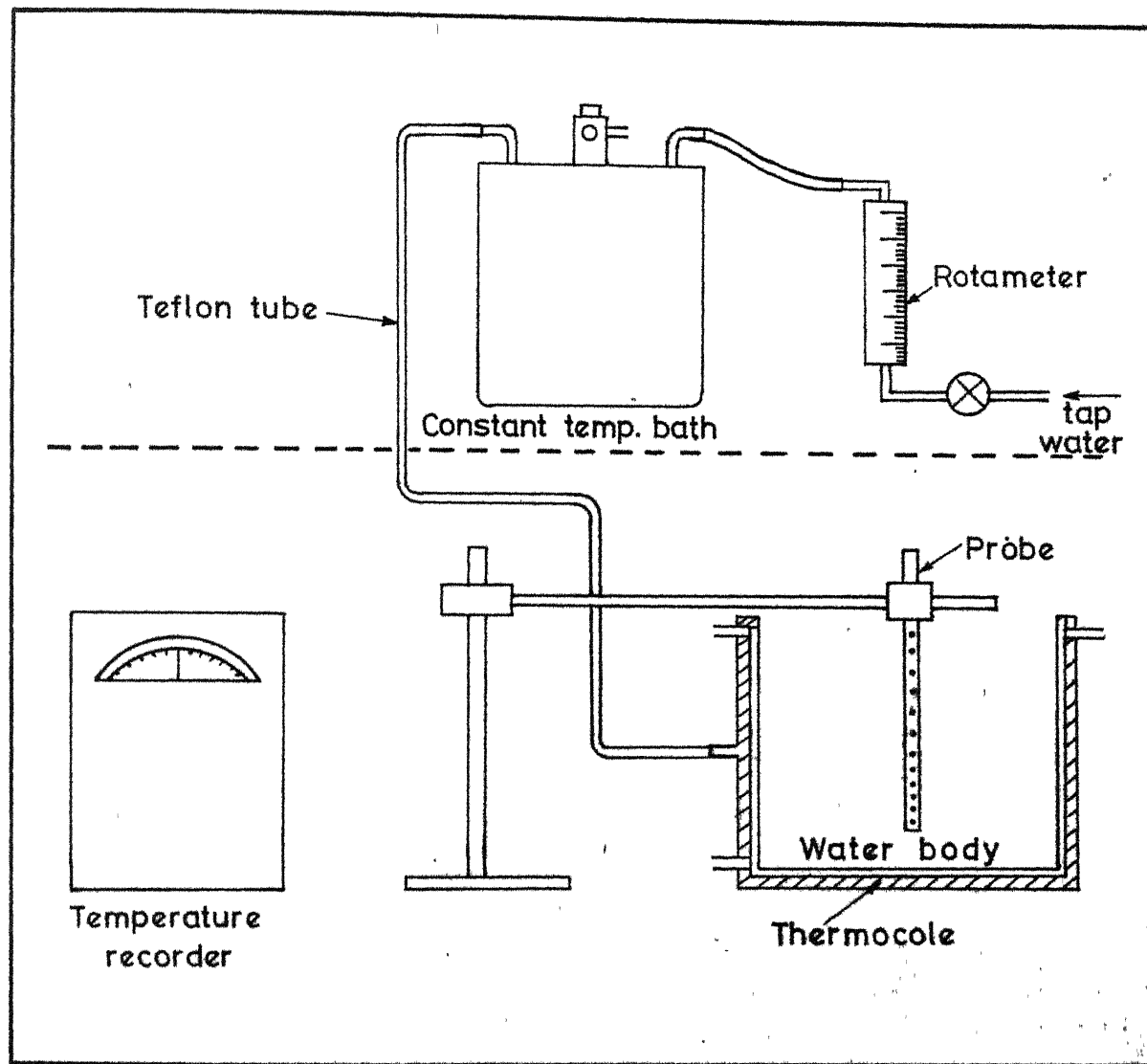


Fig. 2 Schematic diagram of experimental arrangement.

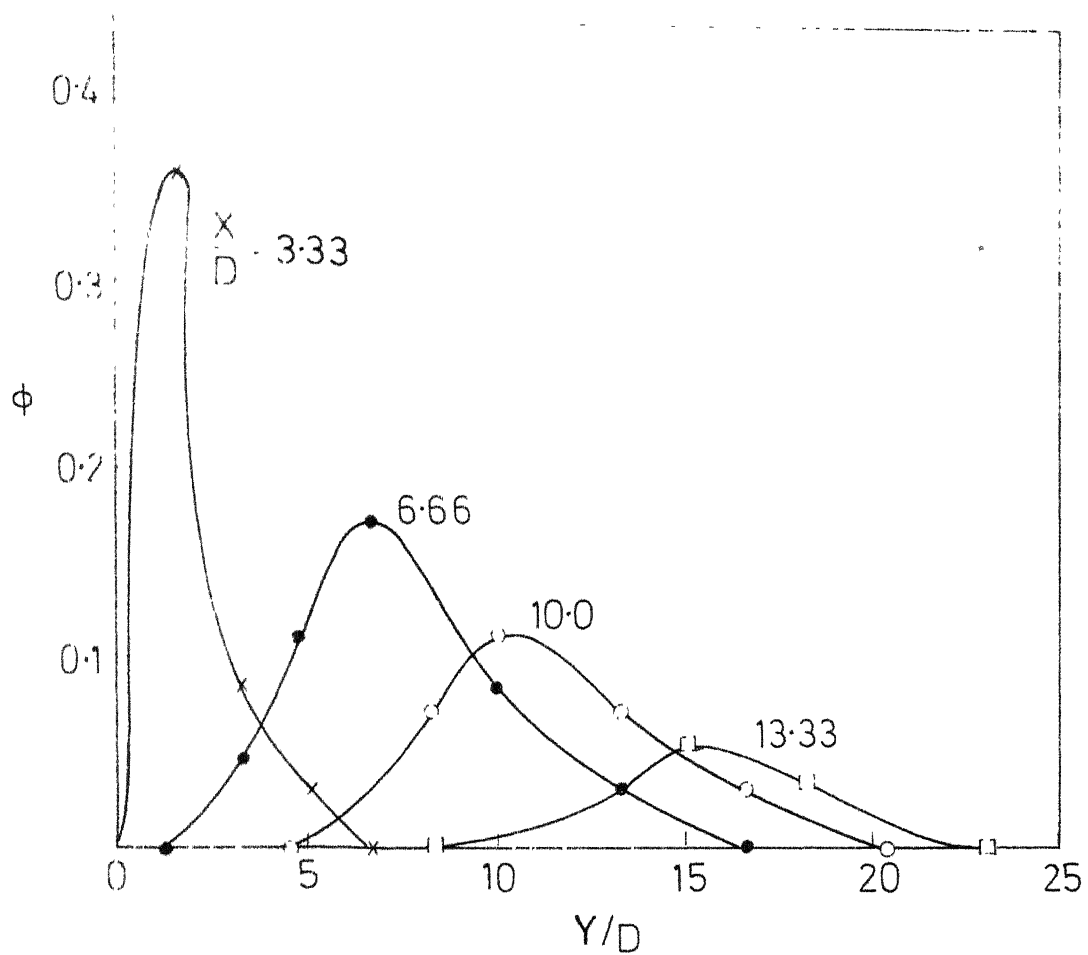


Fig. 3 Temperature profiles with inlet at the centre, with
 $Gr/Re^2 = 0.119$, $Re = 375.4$, $Gr = 1.6739 \times 10^4$

I.I.T. KANPUR
CENTRAL LIBRARY
 Acc. No. A 62160

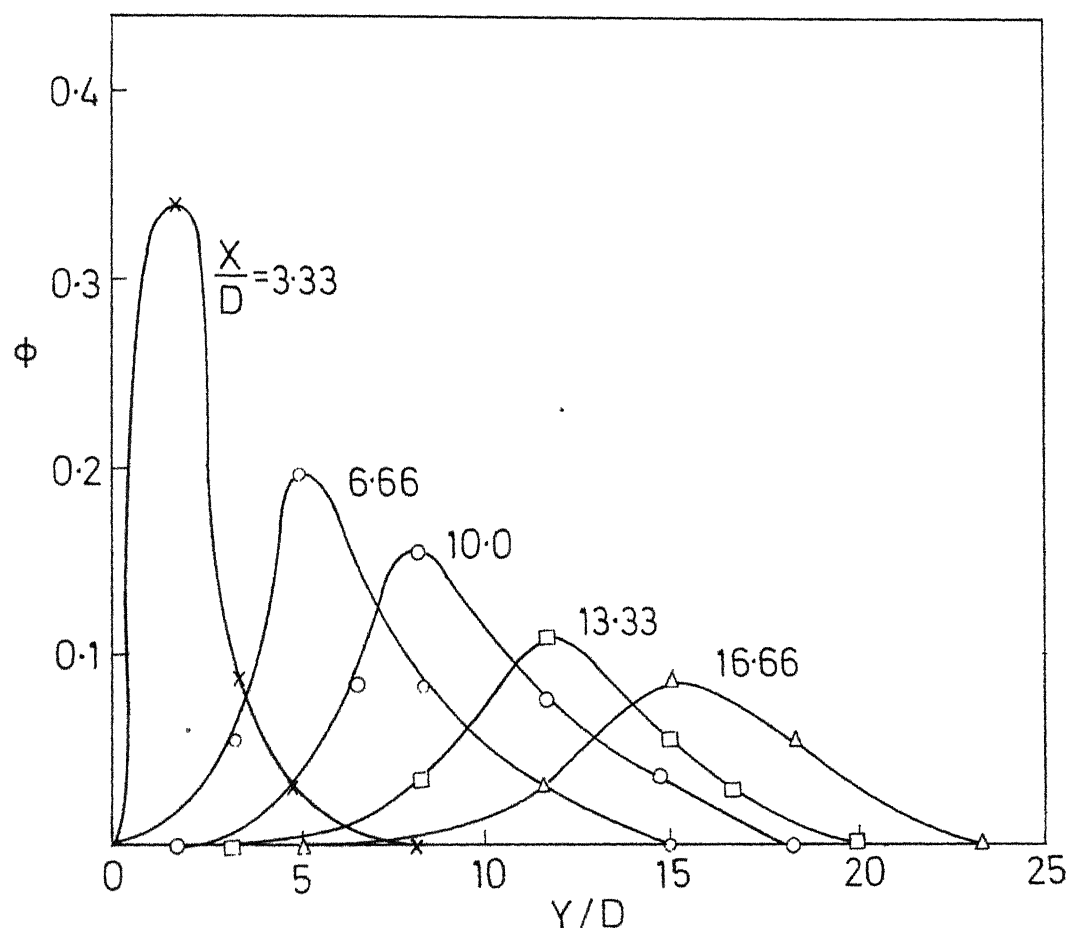


Fig.4 Temperature profiles with inlet at the centre, with
 $Gr/Re^2 = 0.0594$, $Re = 530.6$, $Gr = 1.6739 \times 10^4$

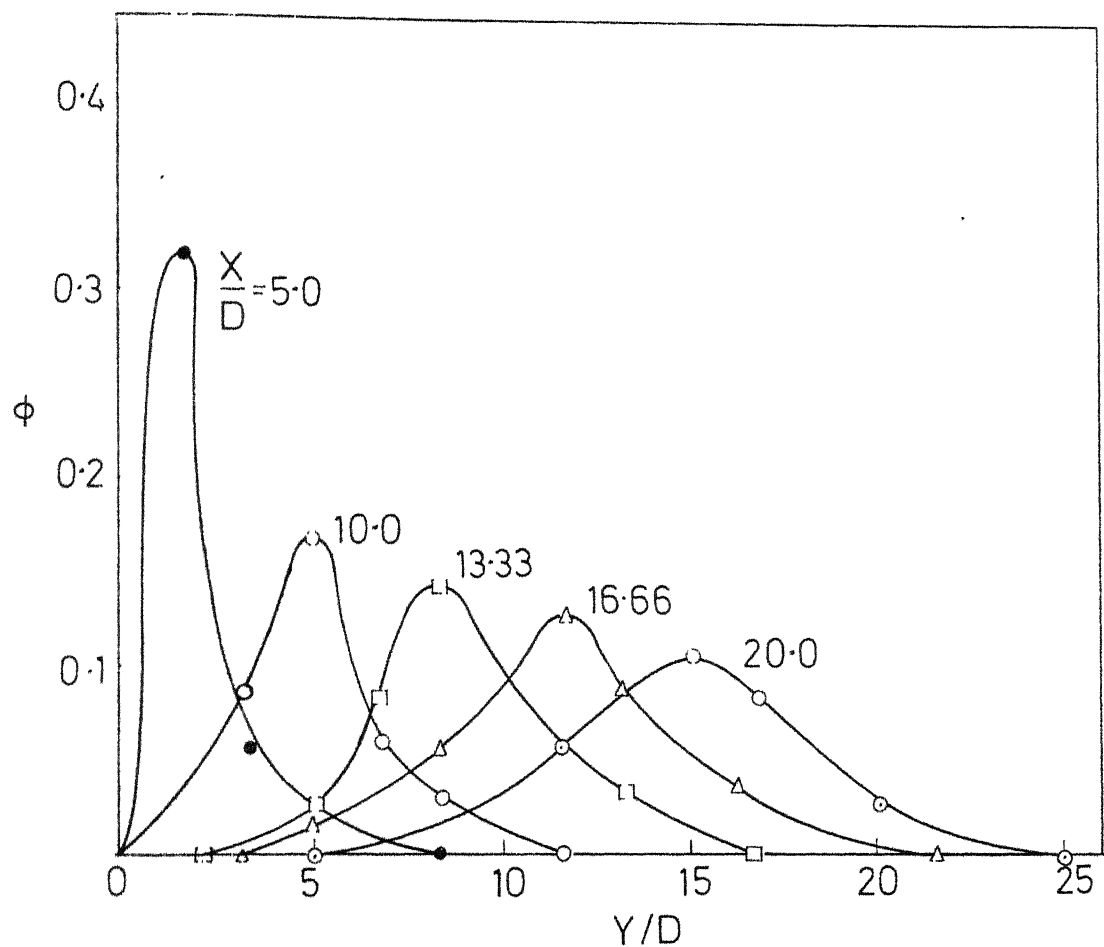


Fig.5 Temperature profiles with inlet at the centre, with
 $\text{Gr}/\text{Re}^2 = 0.02048$, $\text{Re} = 904$, $\text{Gr} = 1.6739 \times 10^4$

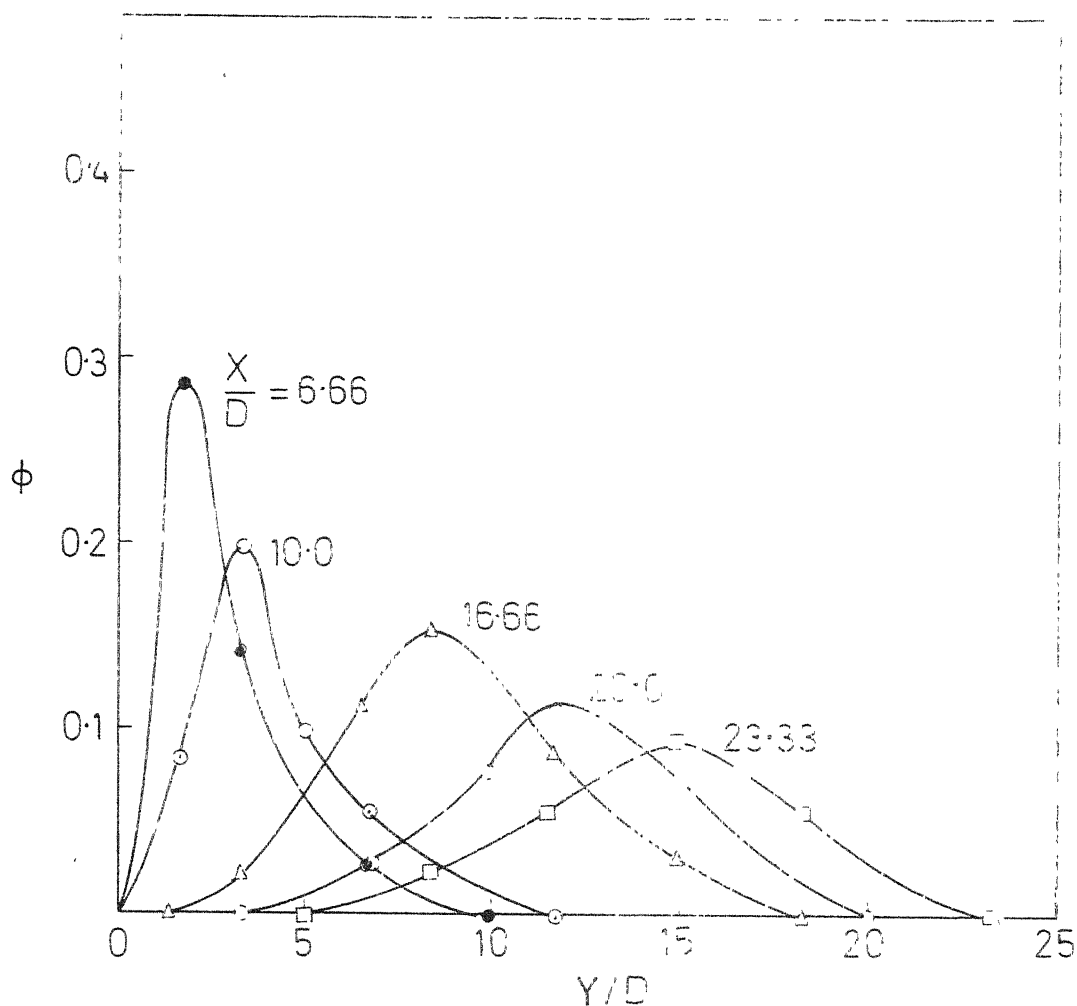


Fig.6 Temperature profiles with inlet at the centre, with
 $Gr/Re^2 = 0.00887$, $Re = 1375$, $Gr = 1.6739 \times 10^4$

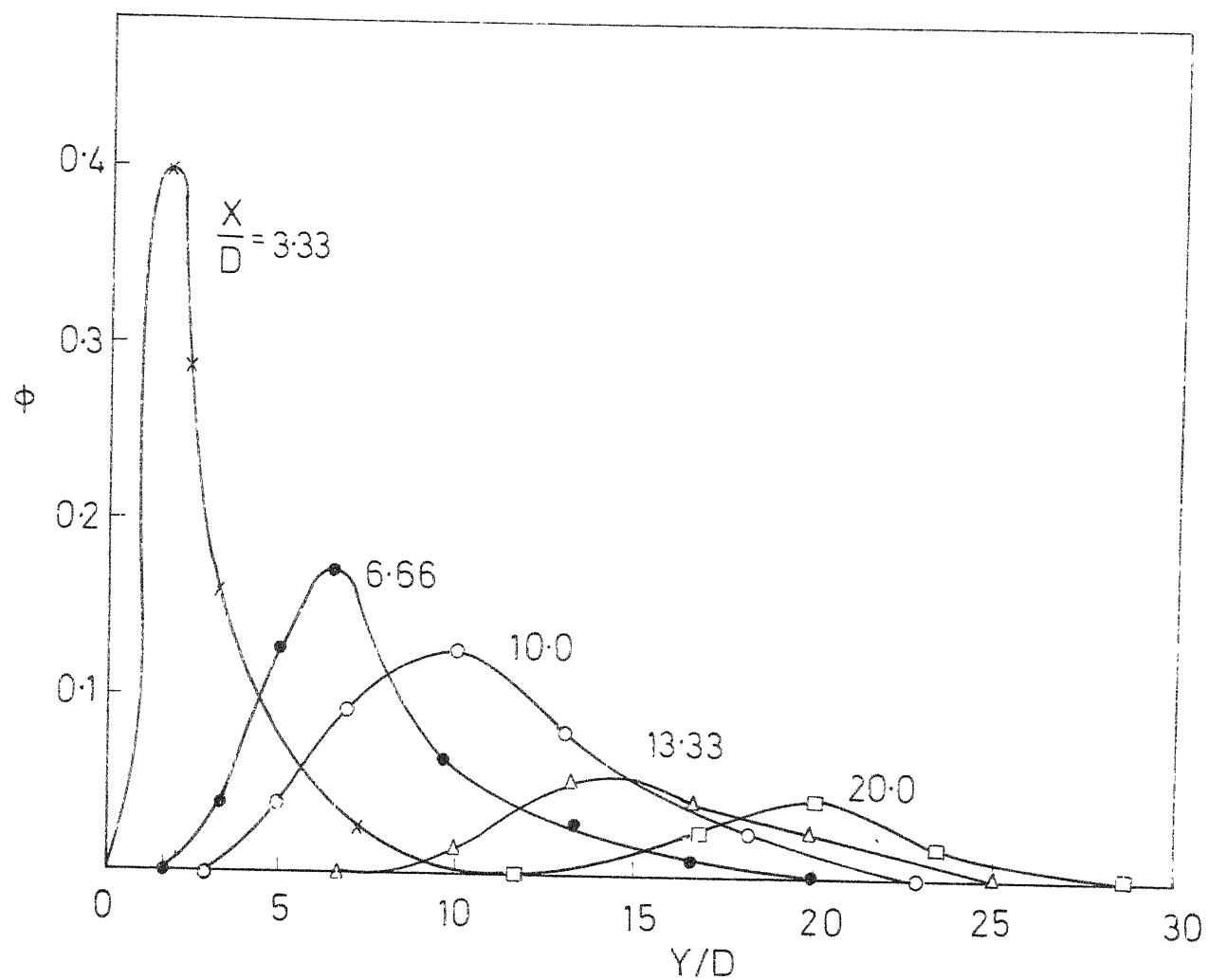


Fig.7 Temperature profiles with inlet at the bottom, with $Gr/Re^2 = 0.0687$
 $Re = 530.6$, $Gr = 1.935 \times 10^4$

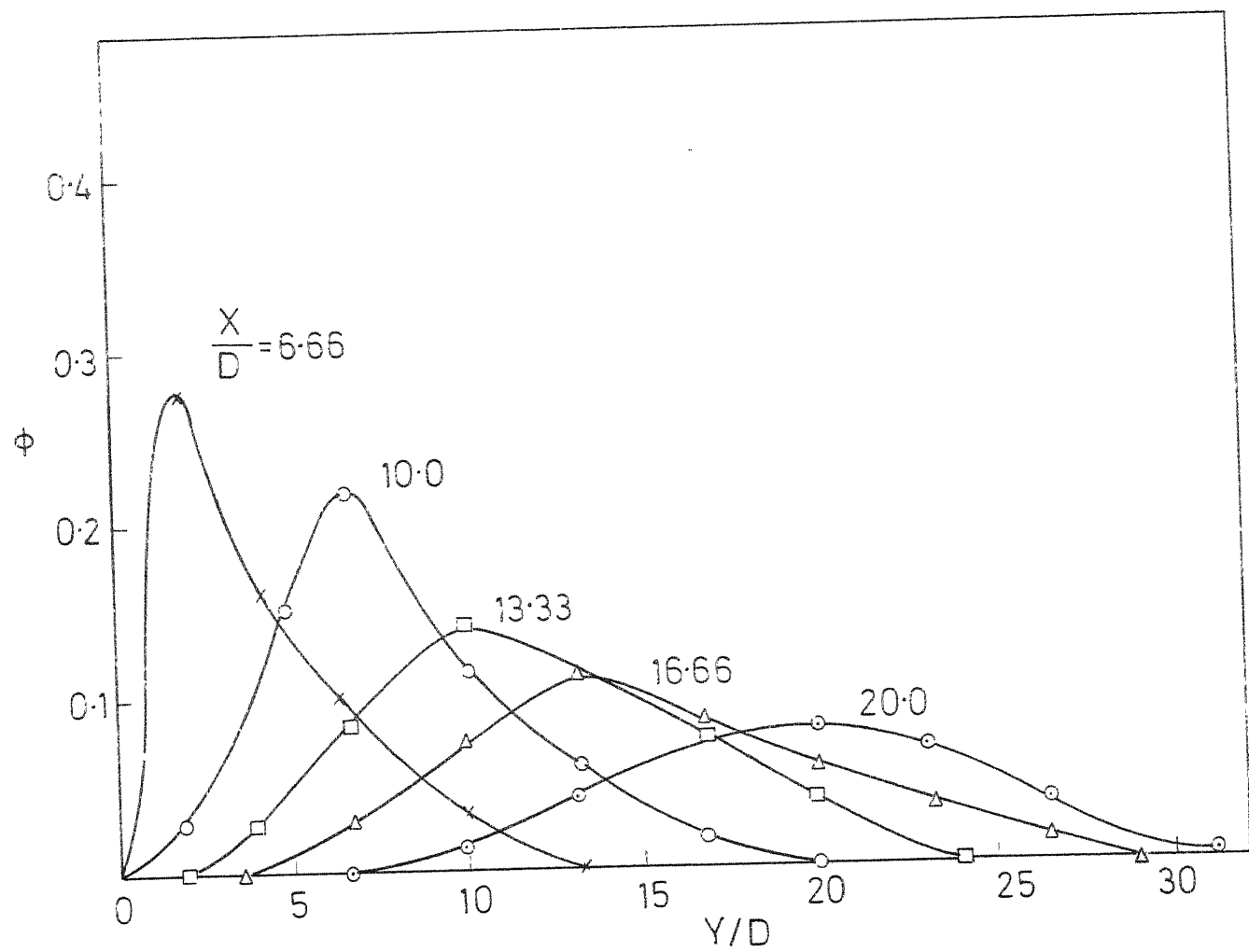


Fig. 8 Temperature profiles with inlet at the bottom, with
 $Gr/Re^2 = 0.02368$, $Re = 904$, $Gr = 1.935 \times 10^4$

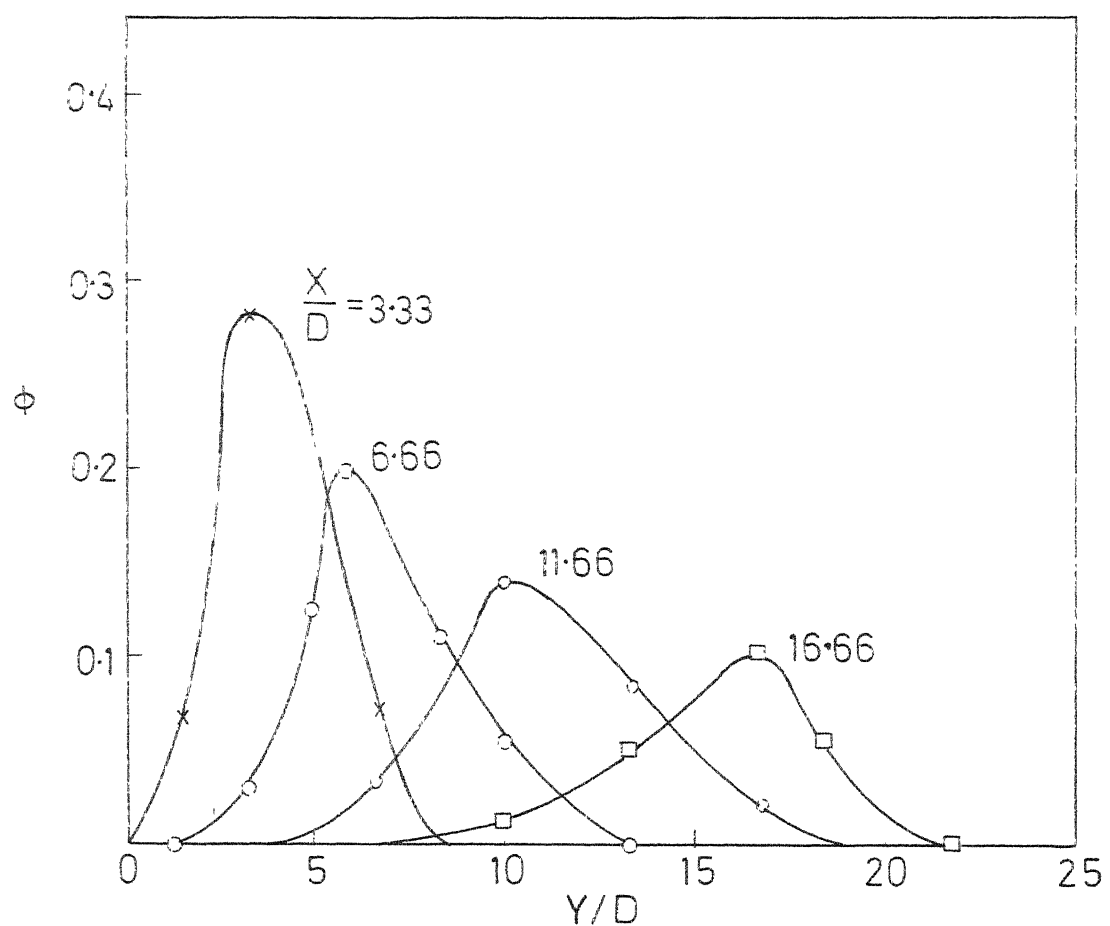


Fig. 9 Temperature profiles with inlet at the bottom, with
 $Gr/Re^2 = 0.0594$, $Re = 530.6$, $Gr = 1.6739 \times 10^4$

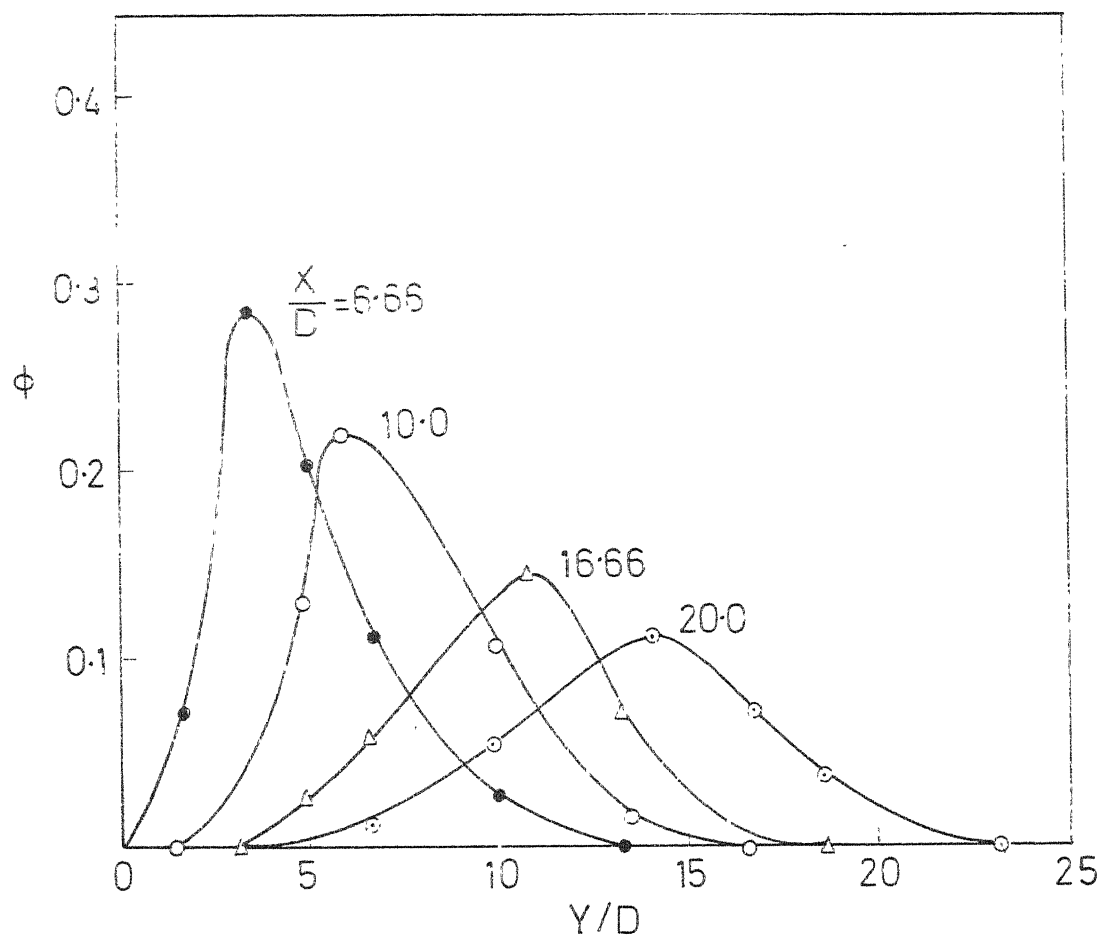


Fig.10 Temperature profiles when inlet at bottom with,
 $Gr/Re^2 = 0.02048$, $Re = 904$, $Gr = 1.6739 \times 10^4$

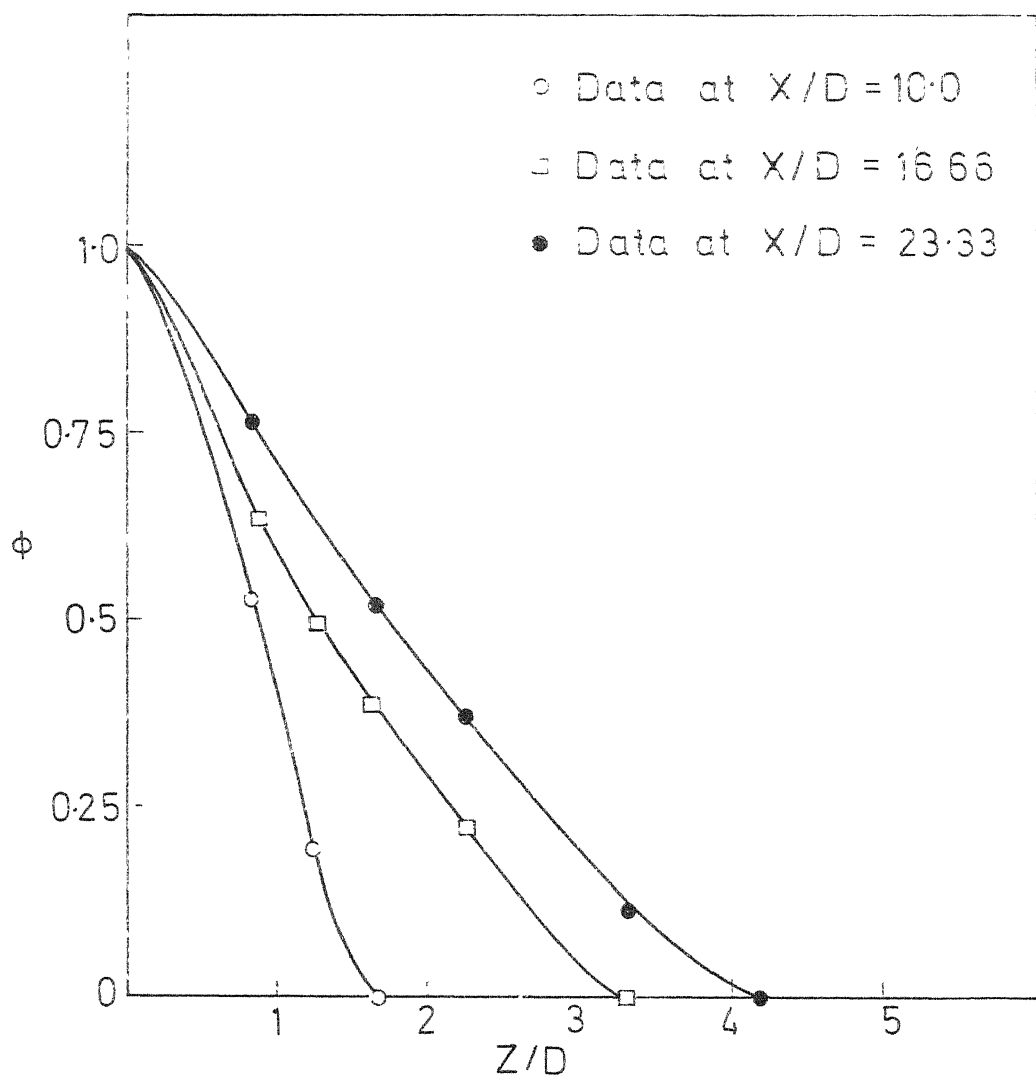


Fig.11 Temperature profiles in the transverse direction for inflow at the bottom, with $Gr/Re^2 = 0.00887$, $Re = 1376$, $Gr = 1.6739 \times 10^4$

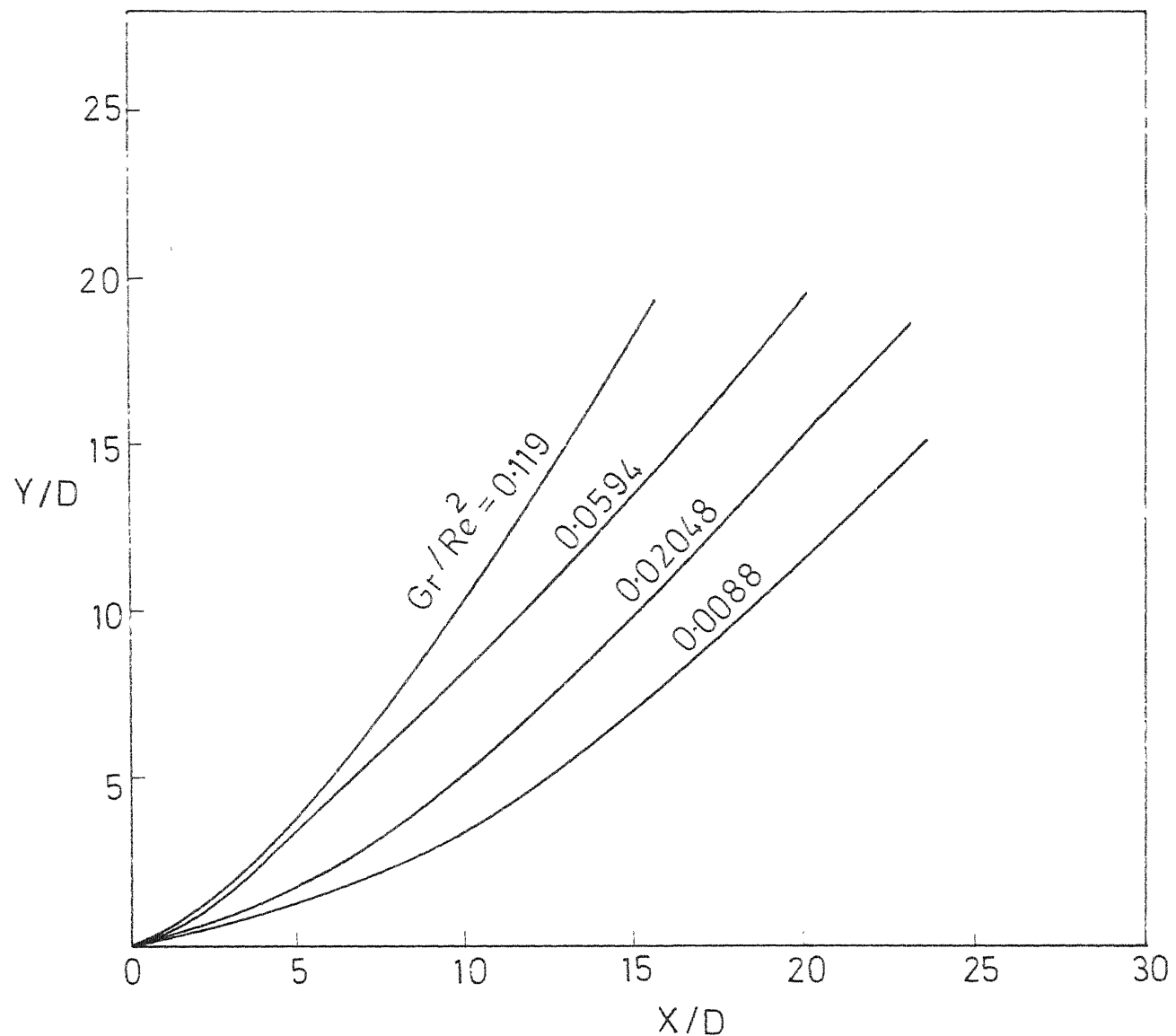


Fig.12 Jet centre-line trajectory with inlet at the centre

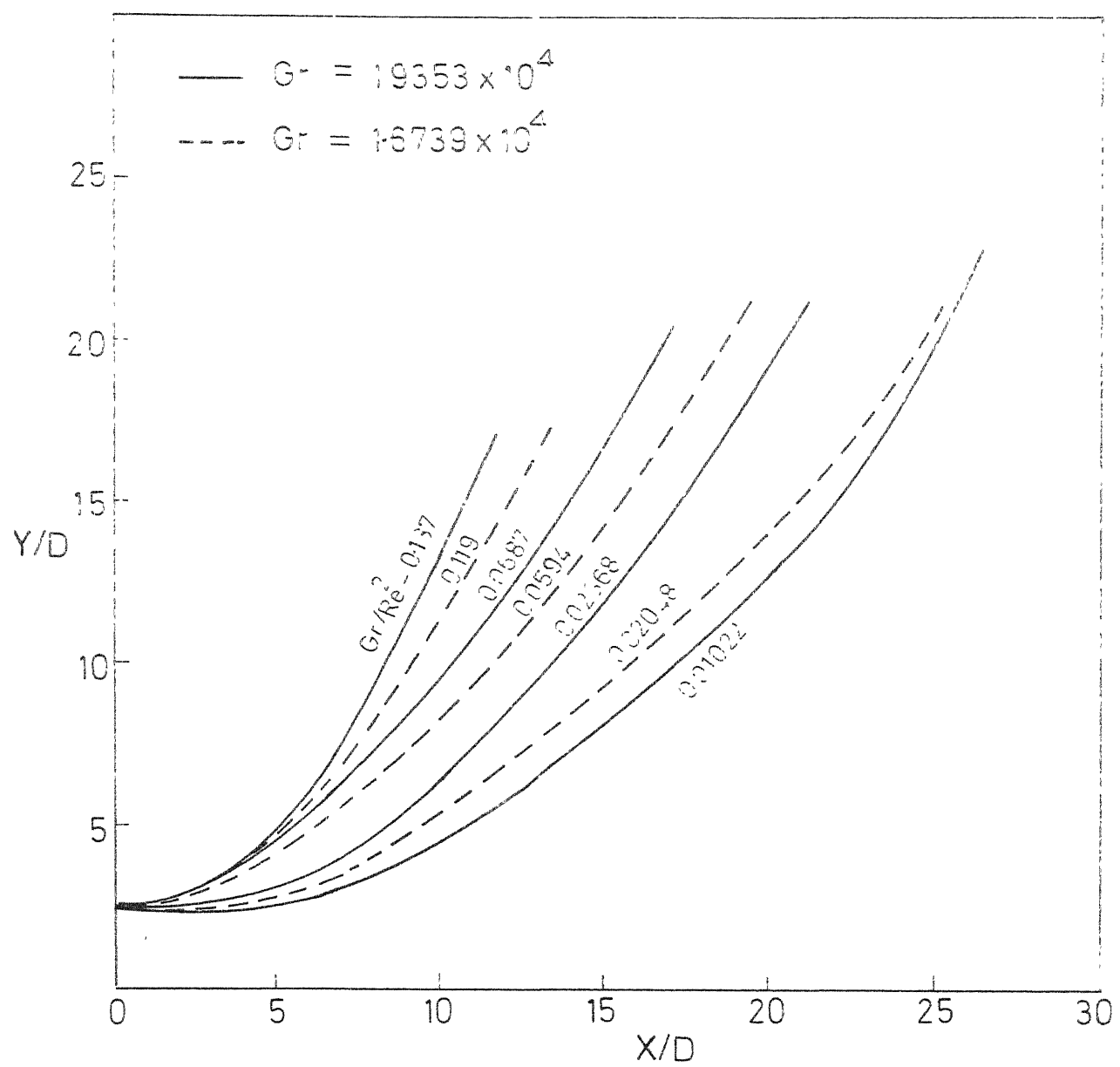


Fig.13 Jet centre-line trajectory with inlet at the bottom

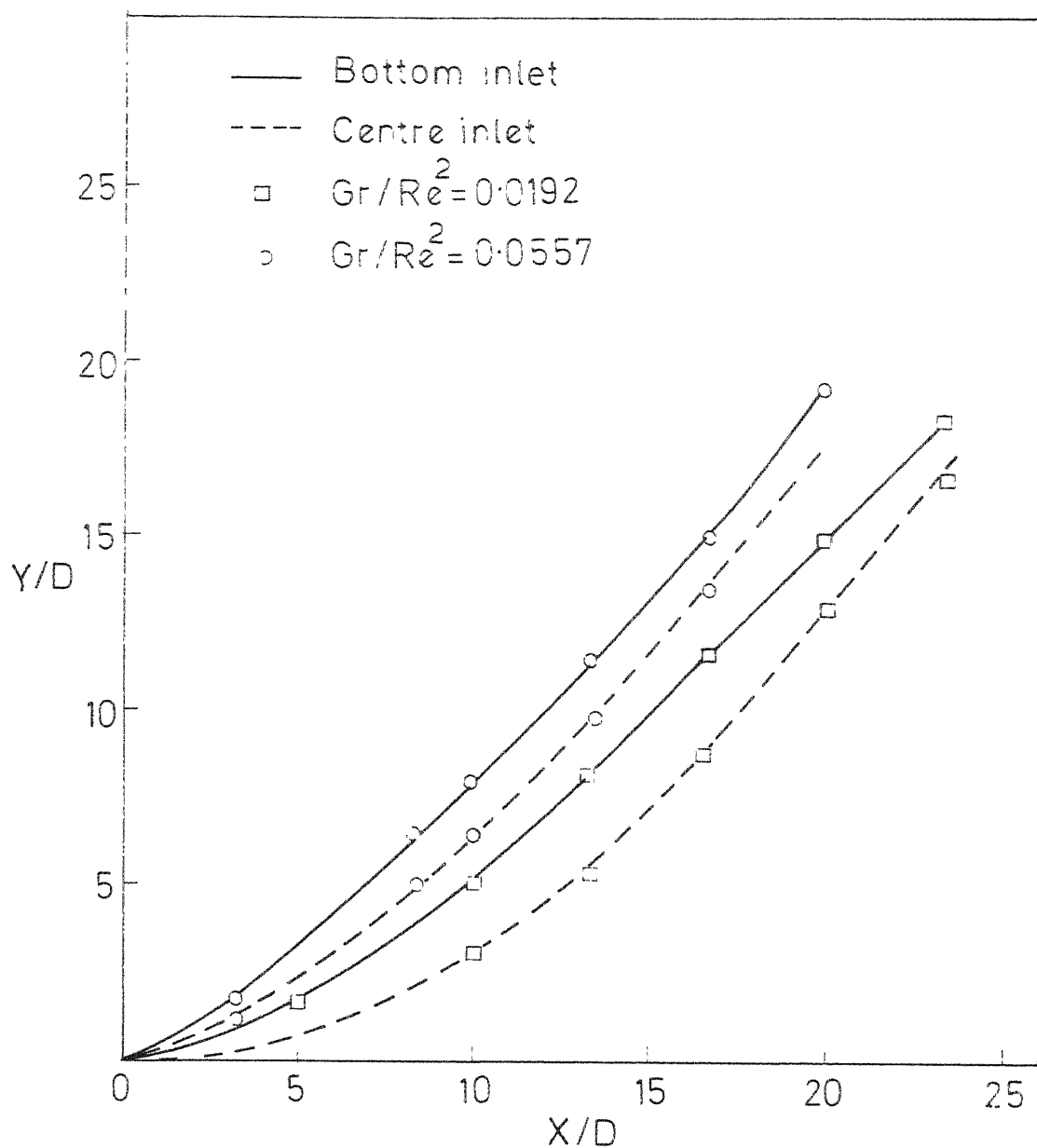


Fig.14 Comparison of the jet centre-line trajectory with inlet at the bottom and at the centre

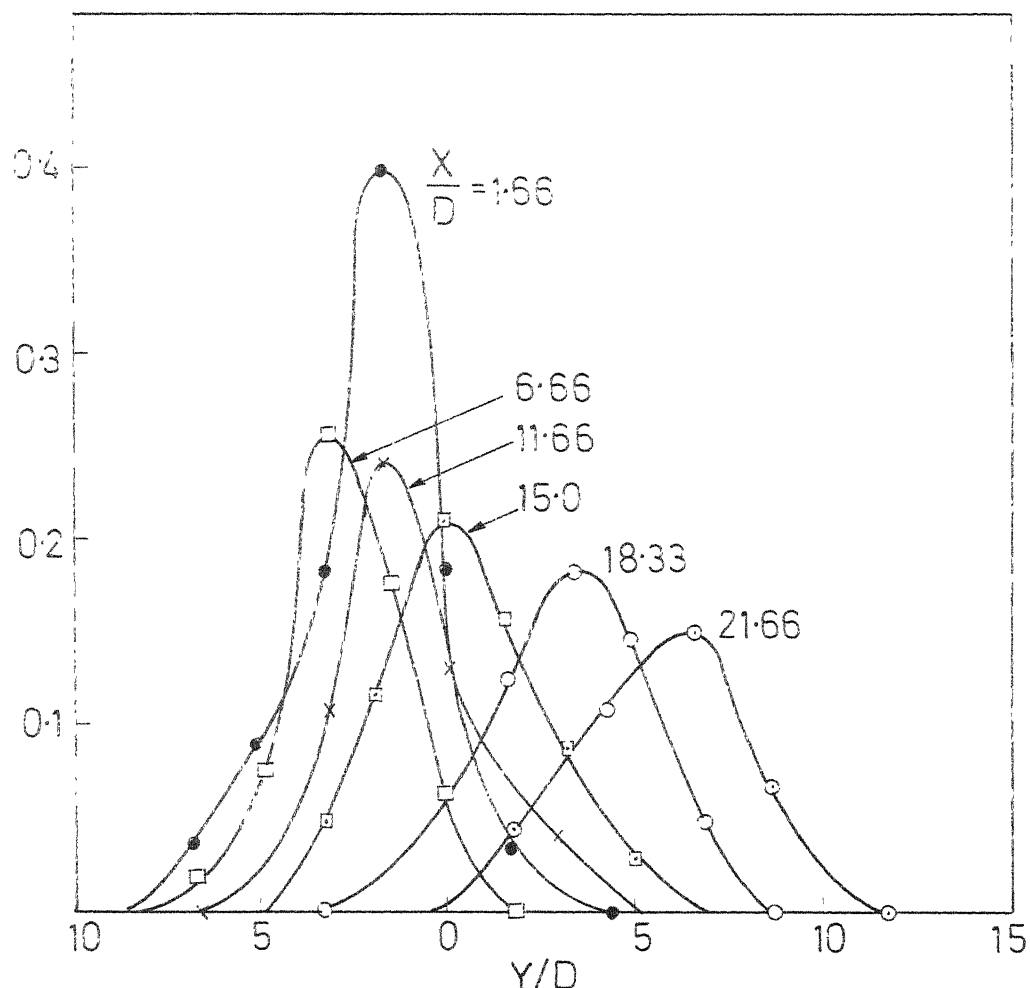


Fig.15 Temperature profiles when jet is inclined at 30° downwards, with $Gr/Re^2 = 0.02048$, $Re = 904$, $Gr = 1.6739 \times 10^4$

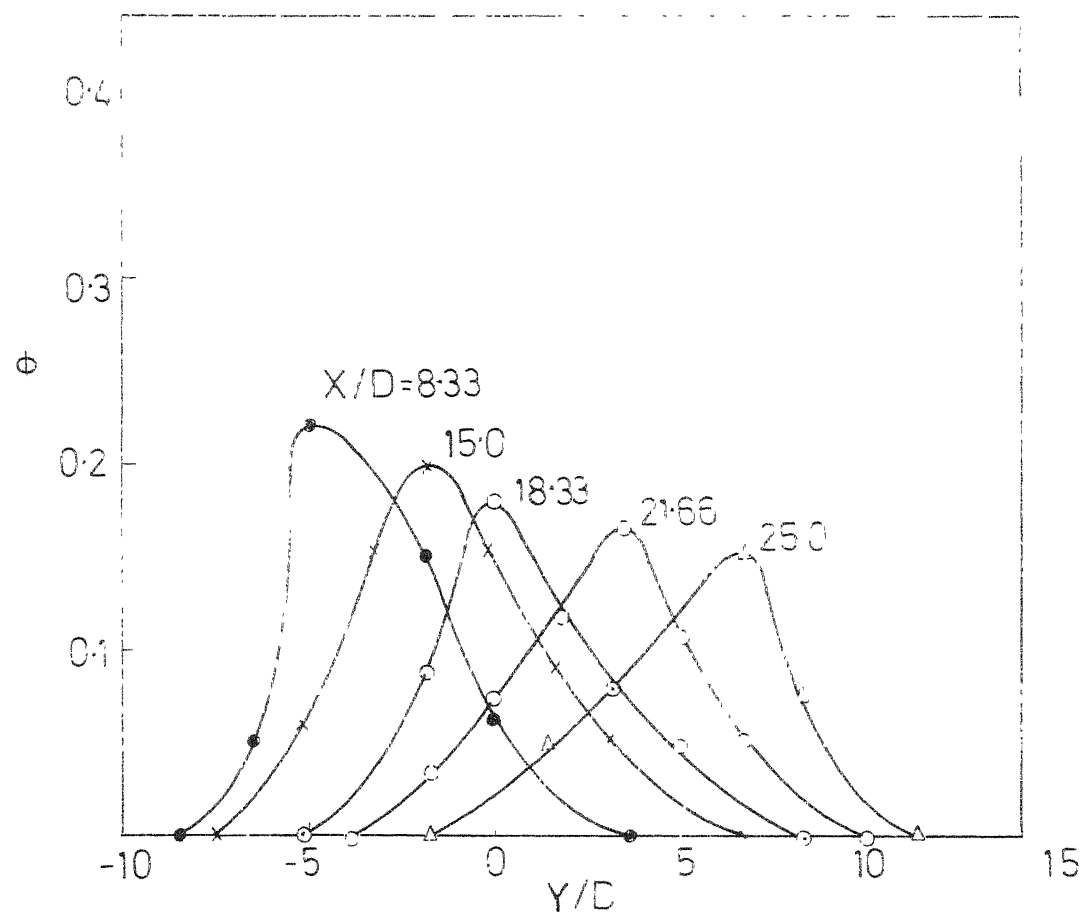


Fig 16 Temperature profiles when jet is inclined at 30° downwards, with $Gr/Re^2 = 0.00887, Re = 1376, Gr = 16739 \times 10^4$

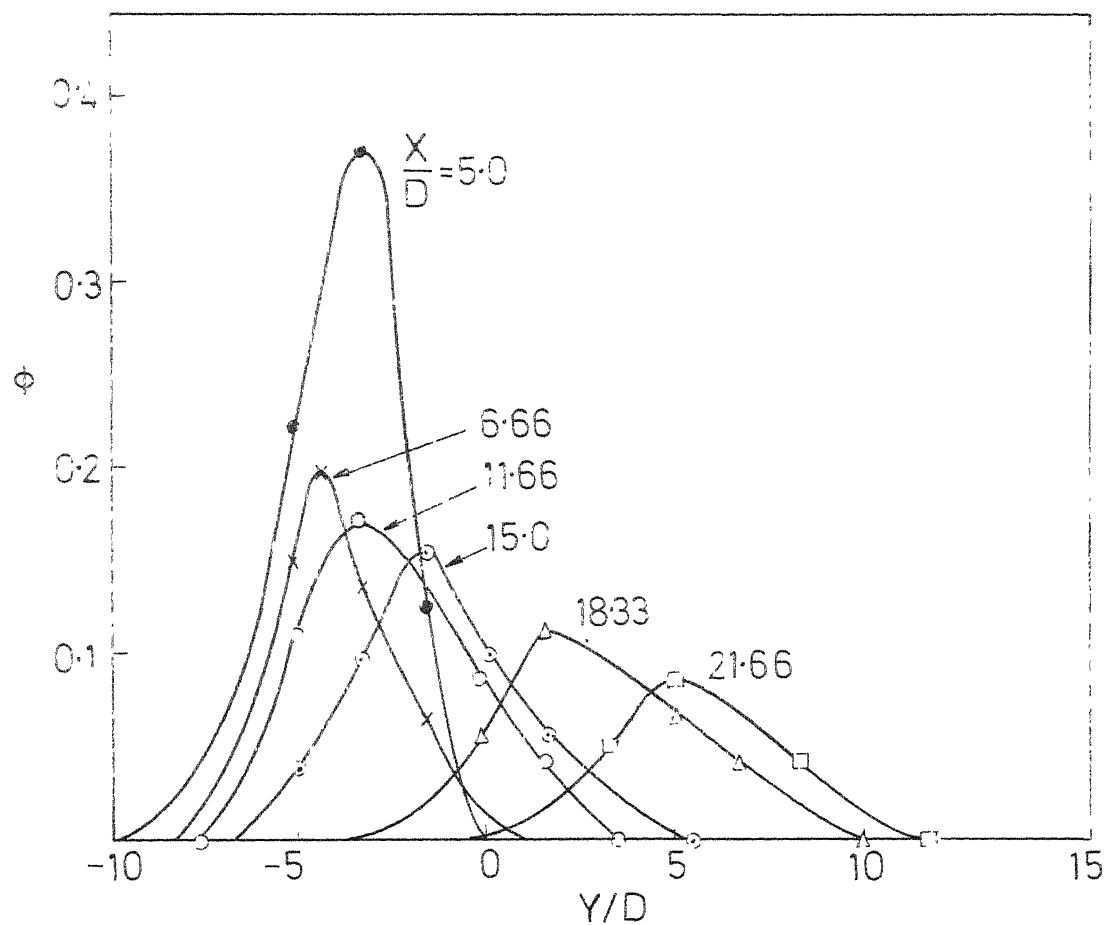


Fig.17 Temperature profiles with jet inclined at 45° downwards,
 with $Gr/Re^2 = 0.02048$, $Re = 904$, $Gr = 1.6739 \times 10^4$

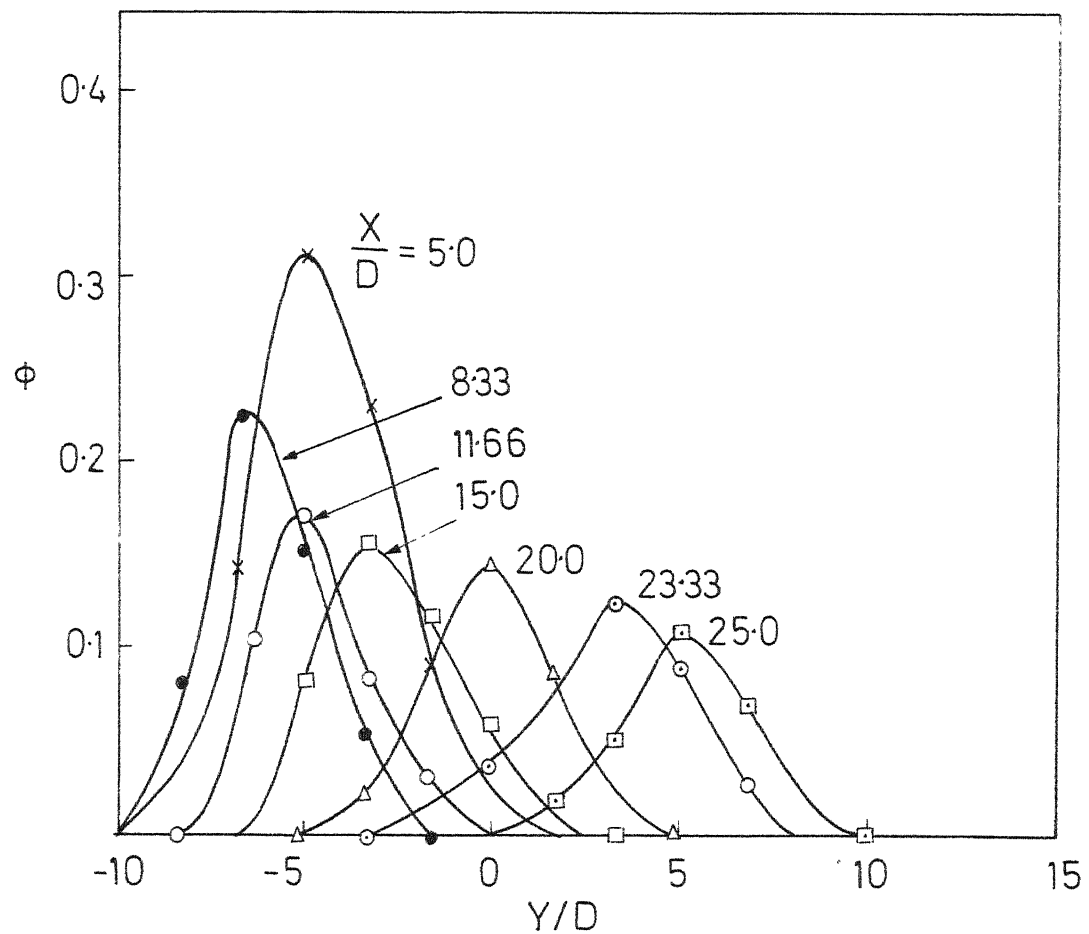


Fig.18 Temperature profiles with jet inclined at 45° downwards,
with $Gr/Re^2 = 0.00887$, $Re = 1376$, $Gr = 1.6739 \times 10^4$

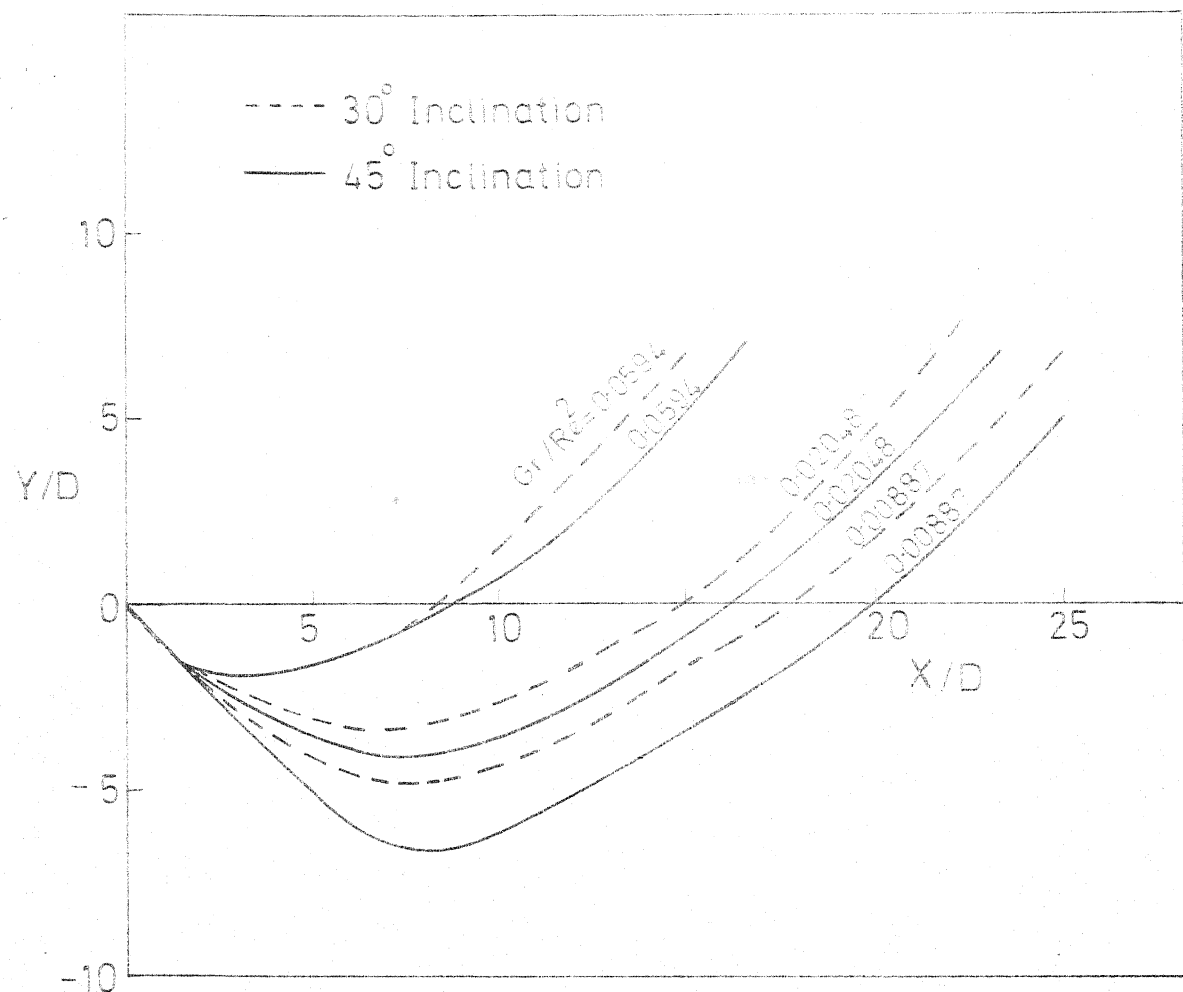


Fig.19 Jet centre-line trajectory with different inclinations

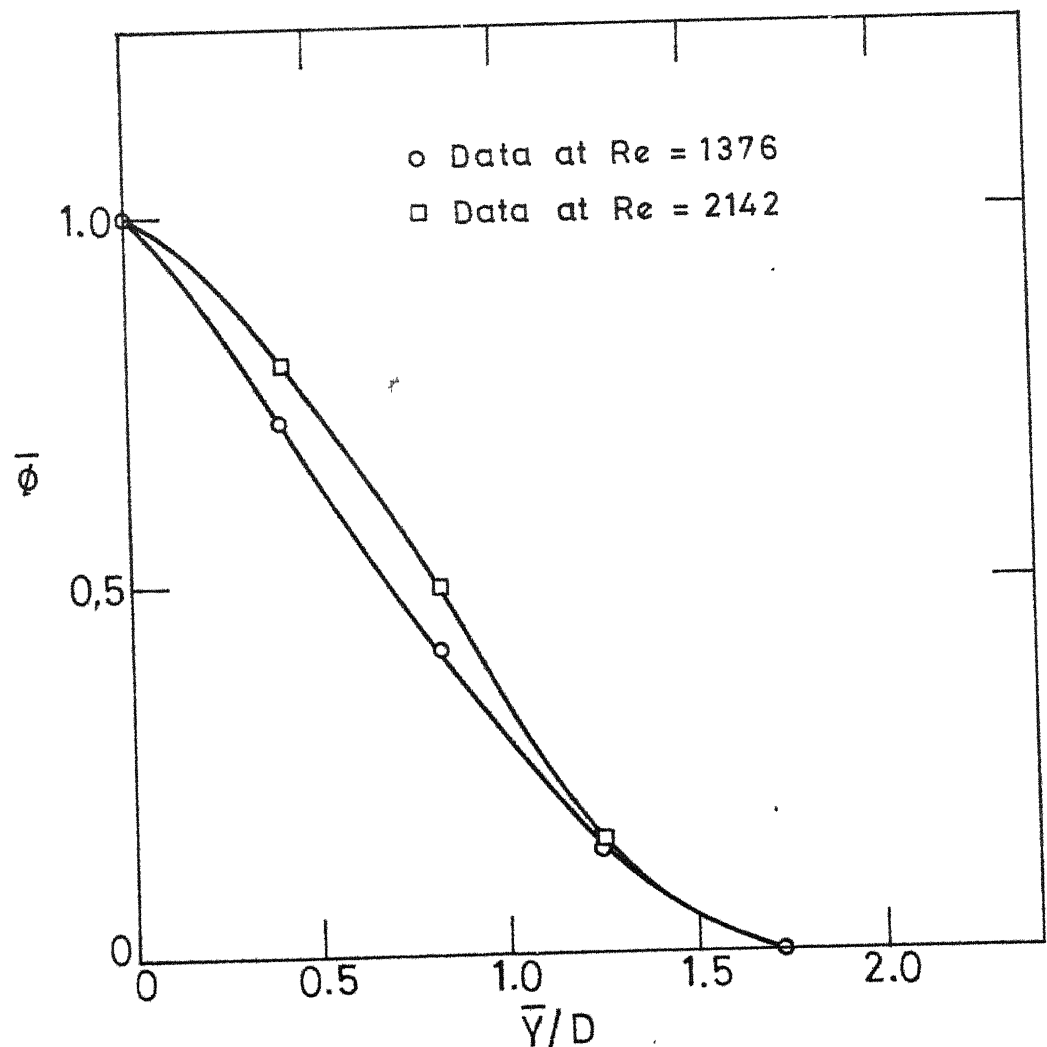


Fig. 20 Temperature profiles for a vertical jet.

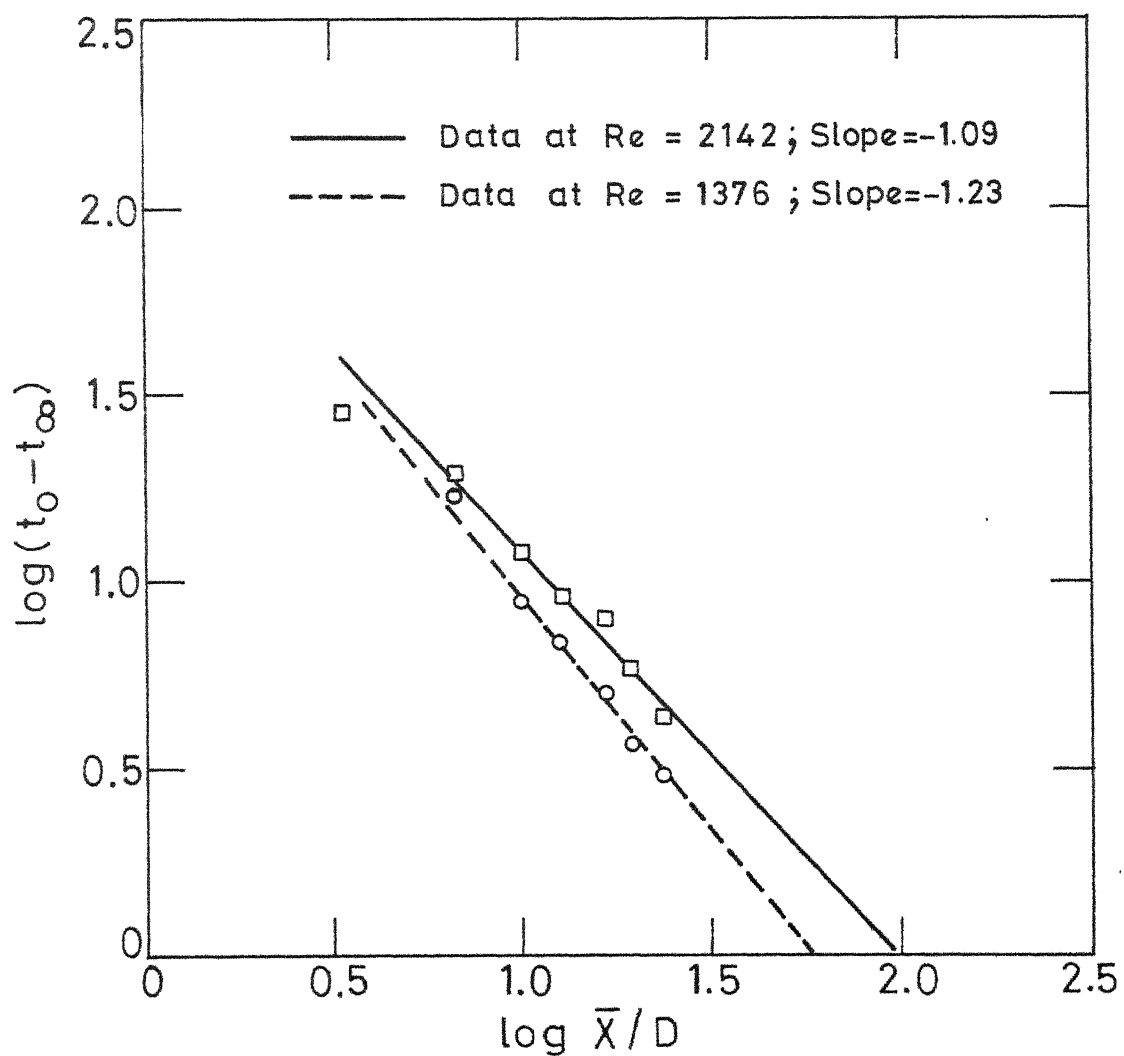


Fig. 21 Center-line temperature vs. vertical height for a vertical buoyant jet.

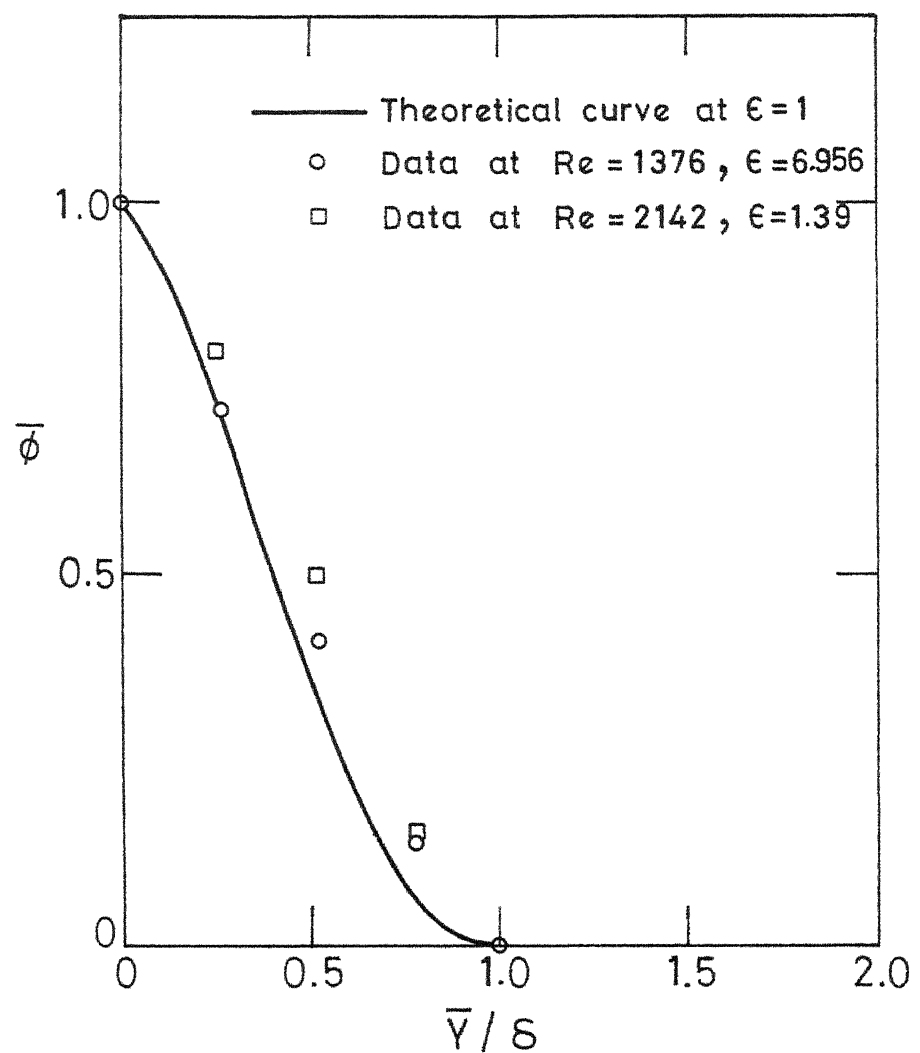


Fig. 22 Comparison between measured temperatures and the theoretical curve for a vertical buoyant jet.

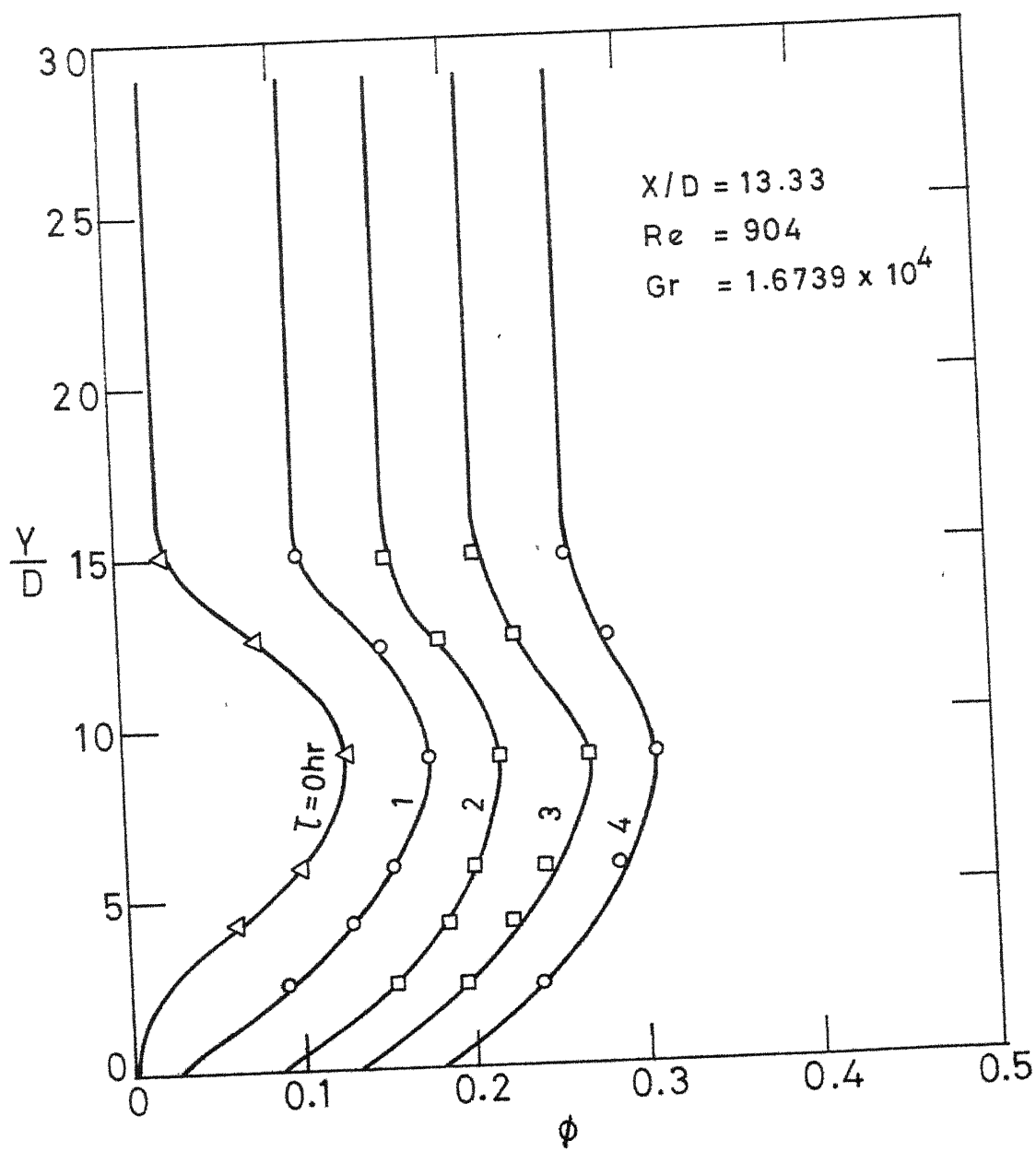


Fig. 23 Temperature profiles of the waterbody in the region of the jet with inflow at the bottom and outflow at the top on the opposite side of the tank.

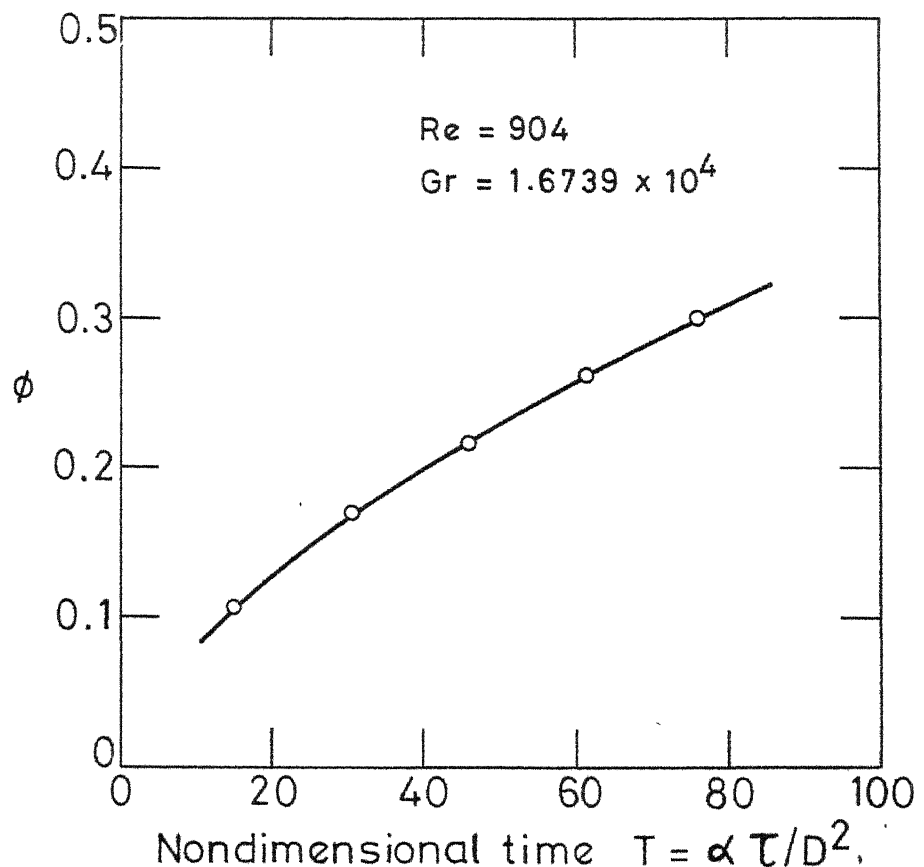


Fig. 24 Transient behaviour of the water body above the jet when the inlet is at the bottom and the outlet at the top on the opposite side of the tank.

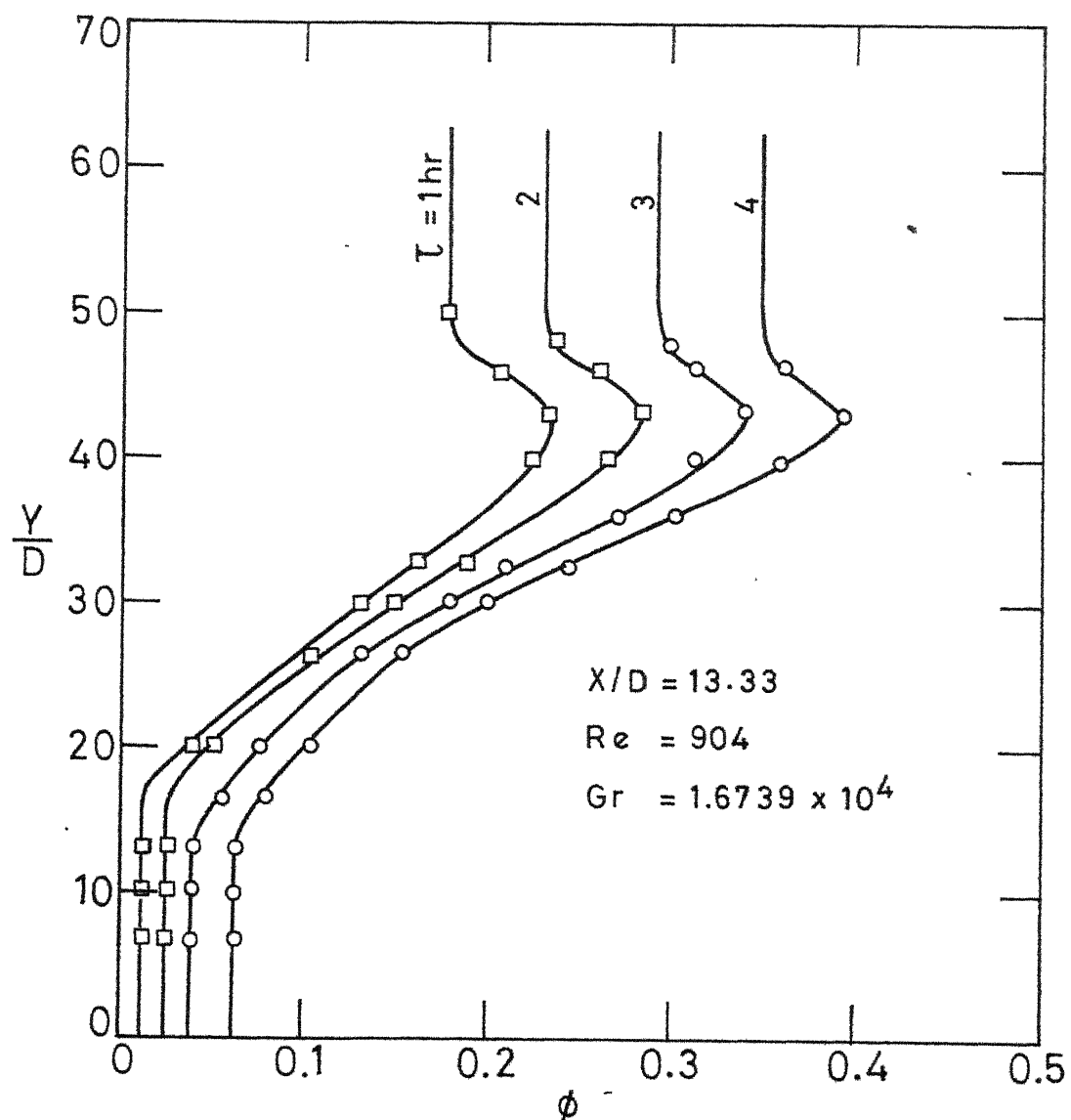


Fig. 25 Temperature profiles of the water body in the region of the jet with inflow at the centre and outflow at the top on the opposite side of the tank

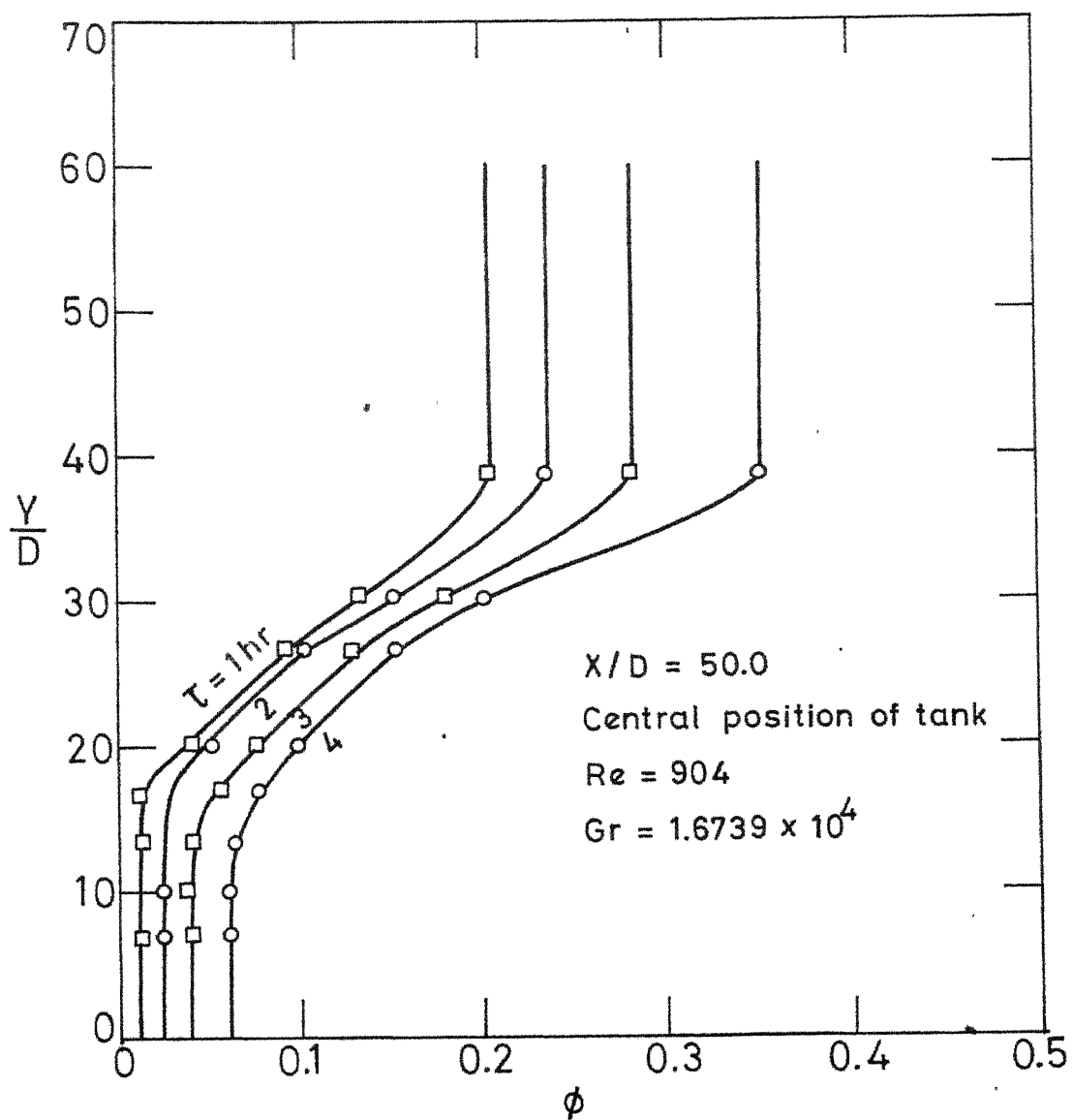


Fig. 26 Temperature profiles of the waterbody in the jet region when the inlet is at the centre and the outlet at the top on the opposite side of the tank.